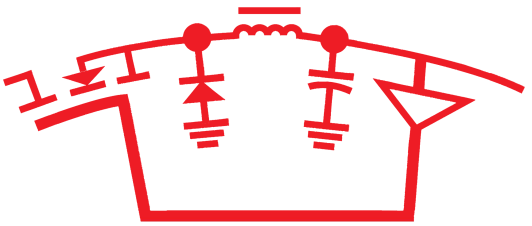

Power Supply Design Seminar

Survey of Resonant Converter Topologies

Reproduced from
2018 Texas Instruments Power Supply Design Seminar
SEM2300,
Topic 1
TI Literature Number: SLUP376

Power Supply Design Seminar resources
are available at:
www.ti.com/psds

Texas Instruments

Survey of Resonant Converter Topologies

Sheng-Yang Yu, Runruo Chen and Ananthakrishnan Viswanathan

ABSTRACT

Starting with 2- and 3-element resonant topology fundamentals, this session walks through the key characteristics, analysis methodology, control challenges and design considerations of resonant topologies. Three design examples demonstrate resonant topology performance with high switching frequency (~1 MHz) or with wide output voltage regulation range (2 to 1 output voltage regulation level). This session also introduces a new resonant topology structure, the CLL resonant converter, with size and efficiency advantages over the traditional LLC series resonant converter. Finally, this session provides guidance on how to select the best resonant topology for various applications.

I. INTRODUCTION

In recent years, resonant converters have become more popular and are widely applied in various applications like server, telecom and consumer electronics. One key attractive characteristic is that a resonant converter can easily achieve high efficiency and allow high frequency operation with their intrinsic wide soft-switching ranges. In addition, magnetic integration, for example, utilizing transformer magnetizing and leakage inductors as two resonant elements, is possible in some resonant converters and allows low component count and cost. However, resonant converters rely on frequency modulation (FM) to achieve voltage or current regulation instead of traditional pulse width modulation (PWM). Therefore, the input-to-output voltage gain of a resonant converter can no longer be derived from the inductor volt-second balance like PWM converters and becomes much more complex than a PWM converter. The complicated input-to-output voltage relation can affect the decision-making process when selecting converter topologies.

This paper aims to provide the audience with a thorough understanding of resonant converters and ease concerns related to the control technique and analytical complexity. Starting from resonant converter fundamentals, this paper walks through the key characteristics, analysis methodology, control challenges and design considerations of resonant converters. A simple and commonly used analysis method for resonant converters, fundamental harmonic analysis (FHA), is introduced along with a classical resonant converter structure. The popular LLC series resonant converter (LLC-SRC) [1] is then used as an example to show the linearization process in FHA. Voltage gains of 2- and 3-element resonant topologies with voltage sources are analyzed in this paper. Three fundamental resonant elements – series resonance (SR), parallel resonance (PR) and notch resonance (NR) – can be found inside these resonant topologies. Each of these three resonant elements contributes different characteristics to a resonant converter.

Beyond the relationship between voltage gain and resonant elements, it is also very important to understand the soft-switching conditions of resonant converters. Circulating current in a resonant converter is used to charge or discharge the parasitic capacitors of the switching elements (e.g. MOSFET) during the switching dead-time, a period that all the switches are turned off. Hence, it is essential to ensure the circulating current is high enough and flows in the desired direction under the desired operation region. In addition to that, enough dead-time must be ensured. A detailed analysis is provided in Section II.

With an understanding of resonant topology fundamentals, detailed analysis of an LLC-SRC is then provided in Section III followed by a high efficiency 1 MHz LLC-SRC design example. LLC-SRC is known to be a good candidate in isolated applications with narrow input and output voltage ranges, such as servers and telecom. A 1 MHz, 390 V to 48 V LLC-SRC design example showcases the strength of LLC-SRC in such

applications and the possibility of pushing the switching frequency higher with a resonant converter while still maintaining high efficiency.

Besides server and telecom equipment, many applications like battery chargers and LED lighting may require their isolated DC/DC power stages to handle wide input or output voltage ranges. In these applications, LLC-SRC might not be a good candidate. Instead, LCC resonant converters provide better overall performance than LLC-SRC in applications with wide input or output voltage ranges. Section IV provides a comparison between LLC-SRC and LCC resonant converters to demonstrate why a LCC resonant converter is a better candidate for wide input or output voltage range applications.

In Section V, a new resonant converter structure is proposed. There are three distinct stages in a conventional resonant converter – switch network, resonant tank and rectifier network. The new structure proposed combines the resonant tank and rectifier network implicitly. That is, one or more resonant elements are placed in the rectifier network stage and participate in the resonance. By doing so, it is possible to improve converter efficiency and size when compared to conventional resonant converters. A new CLL resonant converter is proposed using this new resonant converter structure. Prototypes of LLC-SRC and CLL resonant converters are built to compare the performance. The results show that the CLL resonant converter achieves higher efficiency than LLC-SRC, especially when its switching frequency is higher than the resonant frequencies.

Sections II through V provide a thorough understanding of resonant converter topologies and analysis. In Section VI, resonant converter design challenges and the effects of real life parasitics and parameters are addressed. First, the operational states of a resonant converter are more than a PWM converter. Therefore, synchronous rectifier controller design becomes challenging for a resonant converter. Second, the transient response of resonant converters is addressed with two different resonant converter control strategies: variable frequency control (VFC) and hybrid hysteresis control (HHC). The key component parasitics and their effects on a resonant converter operation are also discussed in Section VI. With the knowledge provided in Sections II through VI, the reader should have clear clues when making resonant topology selection decisions.

II. Resonant Topology Fundamentals

A. Resonant Converter Structure

A conventional resonant converter consists of three sections: a switch network, resonant tank and rectifier network, as shown in Figure 1(a). The switch network generates pulsating voltage or current [2] from a DC voltage or current source and feeds it into the following stage, the resonant tank. On the other hand, the rectifier network receives pulsating voltage or current from the resonant tank and rectifies the pulsating signal into a DC voltage or current. The resonant tank – a two port network formed by inductors (L) and capacitors (C) – modulates its gain amplitude by changing the pulsating signal frequency. In certain switch network and rectifier network combinations, a DC blocking capacitor – C_b in Figure 1(a) – is needed to maintain the inductor volt-second balance, i.e. to avoid saturating the transformer.

Although both the pulsating voltage and current sources are possible candidates as a switch network in a resonant converter, this paper will only focus on resonant converters with switch networks that generate pulsating voltages. A decomposed half-bridge LLC-SRC, shown in Figure 1(b), is used as an example to illustrate how a resonant converter is designed. Series connected MOSFETs in a half-bridge configuration are used as the switch network. With 50% complementary duty-cycle on the series connected MOSFETs, a pulsating signal with peak voltage V_{IN} is fed to the resonant tank. The resonant capacitor, C_r, also serves as the DC blocking capacitor to allow volt-second balance on the resonant inductors. An ideal transformer with central tap output windings is used along with rectifier diodes to generate a DC voltage to the load.

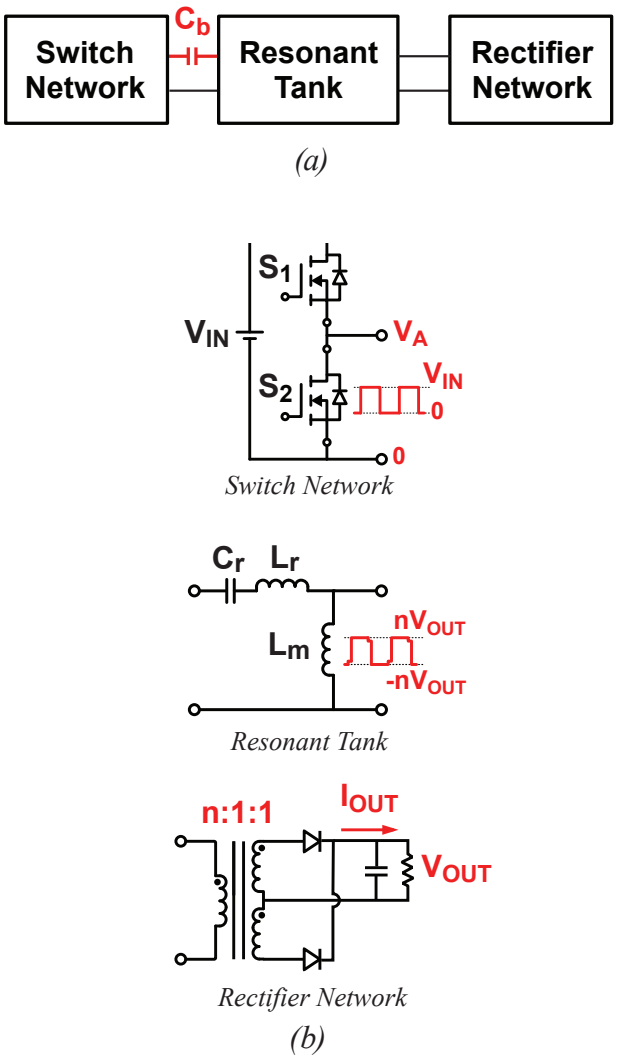

Figure 1 – (a) Conventional resonant converter structure and (b) decomposed LLC-SRC.

B. Fundamental Harmonic Approximation

Although there are many possible control schemes [3] to maintain a resonant converter output regulation, this paper concentrates only on FM – changing the input-to-output gain by only varying the switching frequency with a fixed 50% duty-cycle on the switch network. With FM, a resonant converter input-to-output voltage gain equation becomes very complex as it is frequency dependent. In addition, it is very difficult to analyze a non-linear circuit in the time domain. One commonly used approach is through fundamental harmonic approximation (FHA) to analyze the circuit in the frequency domain.

If we look at the input and output voltages of the half-bridge LLC-SRC resonant tank in Figure 1(b), nearly square waveforms are seen. The voltage harmonics with V_{IN}=390 V are found in Figure 2. It is notable that the fundamental harmonic is the dominant harmonic. In this case, the 3rd harmonic is about 33% of the fundamental harmonic and the total harmonic distortion is about 48% of the input voltage waveform. The output voltage harmonic is also dominated by the fundamental harmonic when the switching frequency is close to the series resonant frequency.

If we only consider the fundamental harmonics on the input and output voltages of the resonant tank and assume the resonant tank output current to be sinusoidal, a resonant converter now becomes

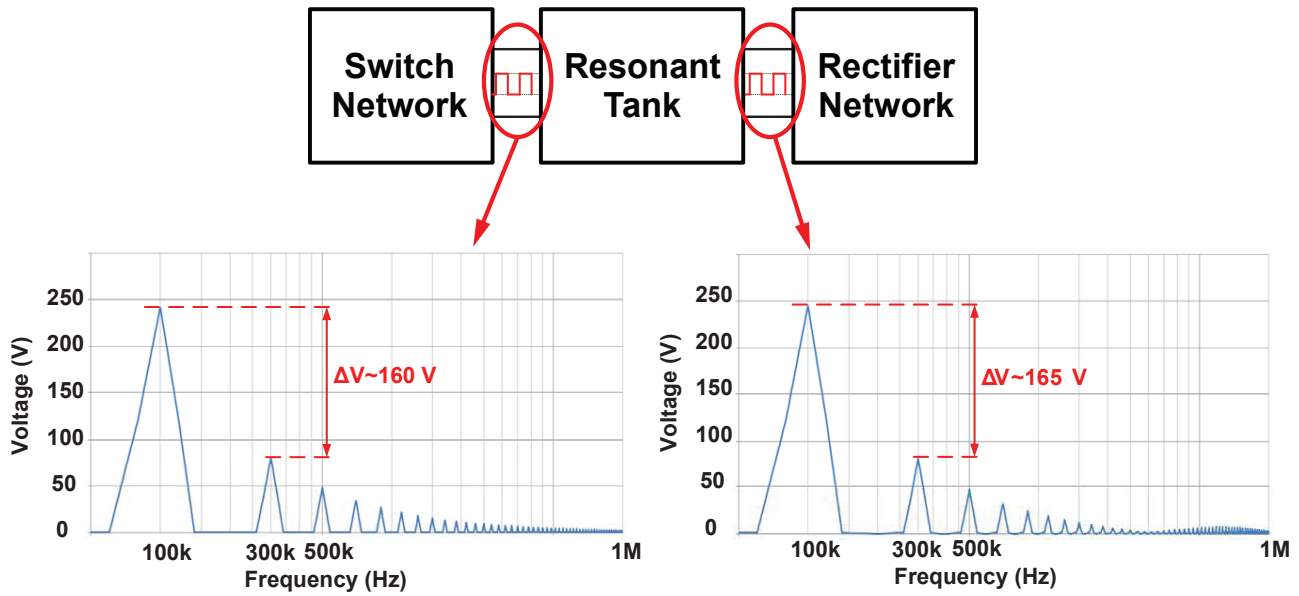

Figure 2 – Resonant tank harmonics.

a linear circuit with a sinusoidal voltage input and resistive output load. Let's use the half-bridge LLC-SRC in Figure 1(b) as an example to demonstrate the FHA linearization process. Starting from the switch network, the output voltage is a pure square wave with a peak voltage V_{IN} and $0.5V_{IN}$ DC content. Since C_r in the resonant tank blocks the DC content, we therefore only need to consider the AC content of the switch network output voltage. The 1st order harmonic of the switch network output voltage, $V_S(t)$, can be expressed as:

$$V_S(t) = \frac{4}{\pi}\frac{V_{IN}}{2}\sin(2\pi f_{SW}t) = \frac{2V_{IN}}{\pi}\sin(2\pi f_{SW}t) \quad (1)$$

where f_{SW} is the switching frequency. Like the switch network output voltage, the rectifier network input voltage 1st order harmonic, $V_{R(1st)}(t)$, can be expressed as:

$$V_{R(1st)}(t) = \frac{4(V_{IN}/2)}{\pi}\sin(\varpi_s t) \quad (2)$$

when operating right on the series resonant frequency. The relationships in (1) and (2) are also illustrated in Figure 3.

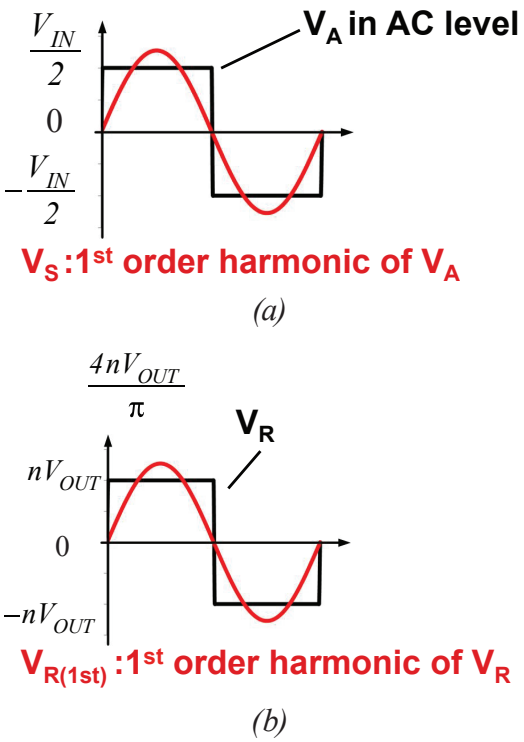

Figure 3 – LLC-SRC resonant tank input and output voltage and harmonics: (a) resonant tank input voltage and (b) resonant tank output voltage.

With a center tap output rectifier stage, each output rectifier diode conducts 50% of the output current. Assume the resonant tank output current, I_R, is a sinusoidal shape, then the amplitude of I_R, $I_{R(PEAK)}$, can be derived using Equation (3):

$$\frac{2}{T_{SW}}\int_0^{\frac{T_{SW}}{2}} I_{R(PEAK)}\sin(2\pi f_{SW}t)\,dt = \frac{I_{OUT}}{n} \quad (3)$$

where T_{SW} is the switching period and n is the transformer turns ratio. Using (3), $I_{R(PEAK)}$ can be found to be $\pi I_{OUT}/(2n)$ and I_R can be expressed as

$$I_R(t) = \frac{\pi}{2}\frac{I_{OUT}}{n}\sin(2\pi f_{SW}t) \quad (4)$$

The I_{OUT} and I_R relationship is also illustrated in Figure 4.

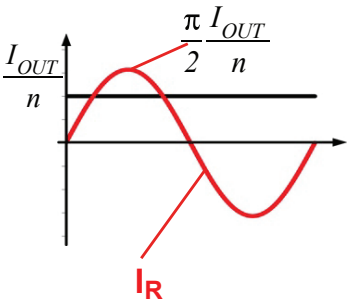

Figure 4 – LLC-SRC resonant tank output current and average load current.

With Equations (2) and (4), the rectifier network can be simplified to an equivalent resistor, R_e, which is expressed as

$$R_e = \frac{V_{R(1ST)}}{I_R} = \frac{8n^2}{\pi^2}\frac{V_{OUT}}{I_{OUT}} = \frac{8n^2}{\pi^2}R_{OUT} \quad (5)$$

With the above FHA process, we can linearize the half-bridge LLC-SRC into the linear circuit in Figure 5 and use simple AC analysis to understand the input-to-output gain. The FHA process is also applicable to other resonant converters with pulsating voltage sources while the level of accuracy may vary.

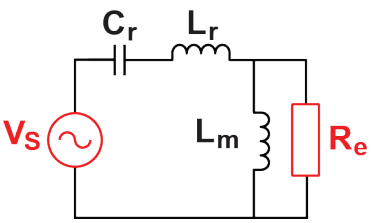

Figure 5 – Linearized LLC-SRC using FHA.

C. Fundamental Resonant Elements

In this section, we are going to focus on understanding the difference between different resonant tanks and how they affect input-to-output gain. D. Huang et al. have systematically analyzed resonant tank characteristics in [4]. Three fundamental resonances – series resonance (SR), parallel resonance (PR) and notch resonance (NR) – are identified to be the fundamental resonances in a resonant tank.

Series resonance has at least two resonant elements connected in series and cascaded between the input and output. A basic SR element and its gain curve are shown in Figure 6. At the resonant frequency, the impedance of the series connected resonant elements becomes zero. Hence, the input-to-output gain is unity. Other than resonant frequency, the input-to-output gain is less than unity. Therefore, SR provides a voltage step-down function like a buck converter.

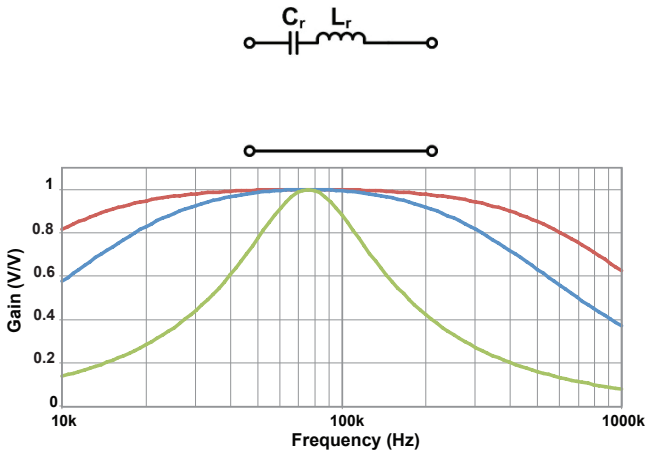

Figure 6 – Basic SR element and its gain curves.

Parallel resonance is formed with at least one inductor and one capacitor. One of these two elements is in parallel with the resonant tank output and the other element is series-connected between the input and output. Basic PR elements and their gain curves are shown in Figure 7. Around the resonant frequency, the voltage gain can be very high. Therefore, a PR can be used in applications that need a voltage step-up function, like a boost converter. It is also notable that when a PR has its capacitor in parallel with the output port, the voltage gain at high frequency drops to zero because the capacitor impedance becomes zero. This implies that the output short circuit protection can be achieved by just increasing the switching frequency with the output port parallel capacitor PR.

Notch resonance is formed either with an LC in parallel and placed in series between the input and output or with an LC in series and placed in parallel with the output. Basic NR elements and their gain curves are shown in Figure 8. The parallel LC in NR element #1 in Figure 8(a) becomes an open circuit at the LC resonant frequency; therefore, voltage gain becomes zero at the resonant frequency. The cascaded LC in NR element #2 in Figure 8(b) becomes a short circuit at the LC resonant frequency and leads to zero gain at the output at the resonant frequency. With the open and short circuit characteristics that NR elements have, NR creates a valley in the gain curve as shown in Figure 8(c). A valley in the middle of the gain curve is generally undesirable because it requires a complicated controller design.

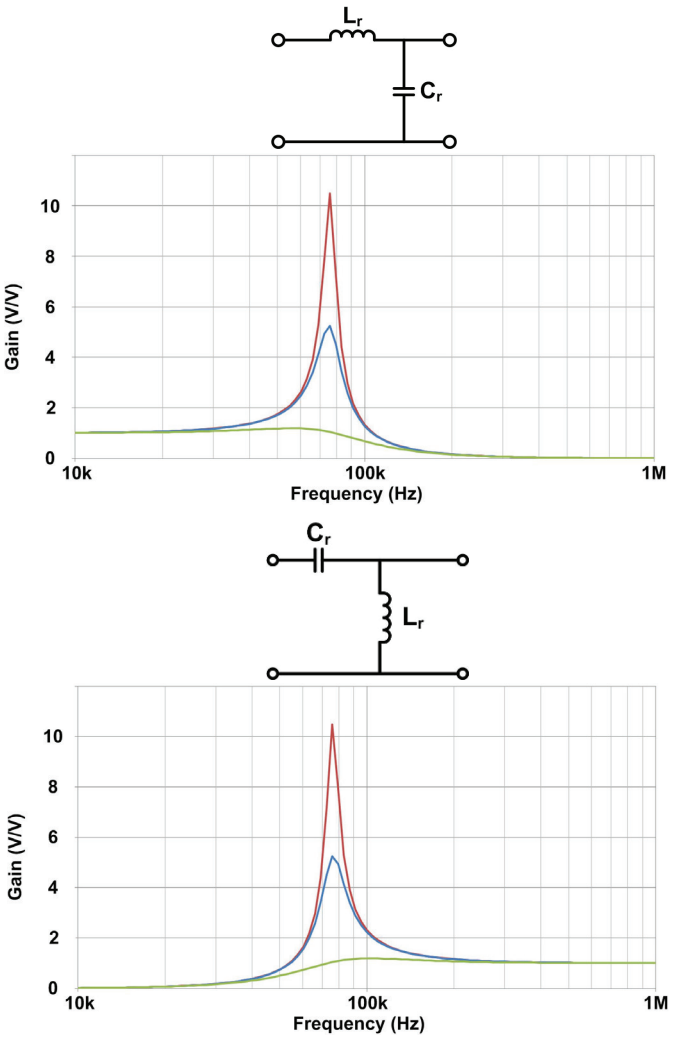

Figure 7 – Basic PR elements and their gain curves.

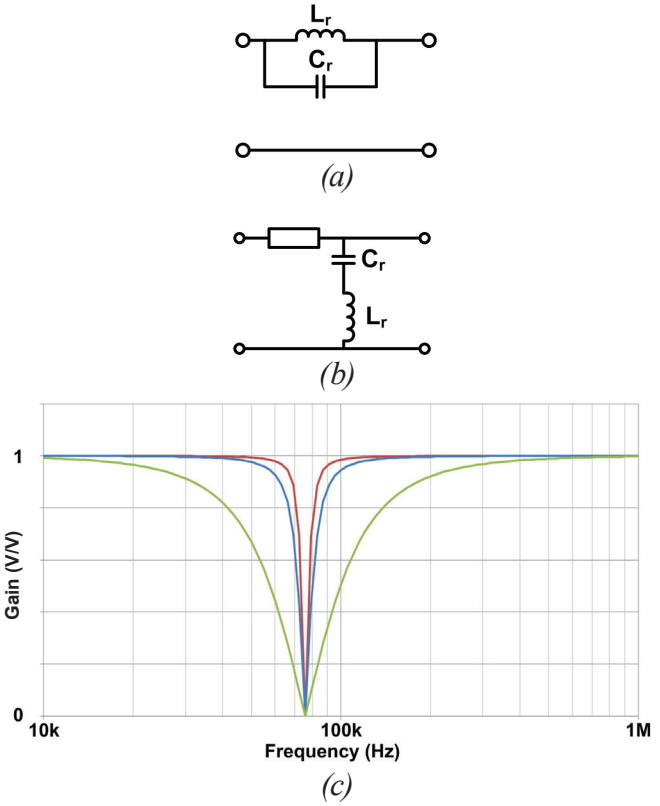

Figure 8 – Basic NR elements and their gain curves: (a) basic NR element #1, (b) basic NR element #2 and (c) gain curves of NR element #1.

It is also notable that there is a series element in Figure 8(b). The series element, an inductor or a capacitor, is required to work with NR element #2 or the input and output will be shorted together. Because of the series element, NR element #2 will have both NR and PR characteristics at the same time. One example is illustrated in Figure 9 with PR and NR effects highlighted on the gain curves.

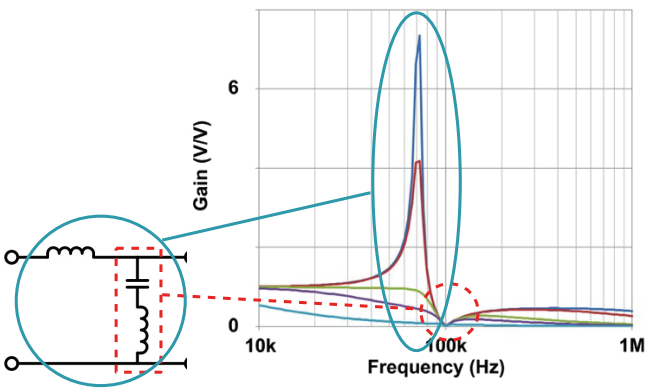

Figure 9 – NR element #2 with inductor as series element.

D. 2- and 3-Element Resonant Topologies

With an understanding of the fundamental resonant elements, it is now easy to walk through the characteristics of resonant tanks [5]. There are eight possible resonant tank combinations in 2-element resonant topologies, as shown in Figure 10.

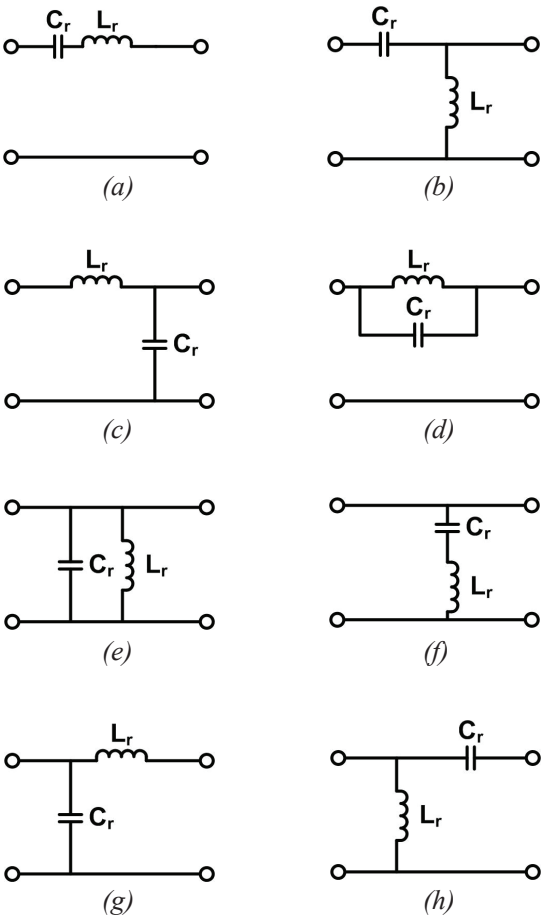

Figure 10 – Possible 2-element resonant tanks: (a) tank A, (b) tank B, (c) tank C, (d) tank D, (e) tank E, (f) tank F, (g) tank G and (h) tank H.

Tank A is a series resonant converter with SR. Tanks B and C are parallel resonant converters with PR. Tank D is a resonant converter with NR, as illustrated in Figure 8. It is worth noting that both tanks E and F lack voltage regulation capability because the input is directly connected to the output. In addition, both tanks E and G require a pulsating current source, which is not in the scope of this paper. The inductor in tank H is clamped by the input voltage and does not participate in resonance. Therefore, tanks A through D are truly 2-element resonant converter candidates.

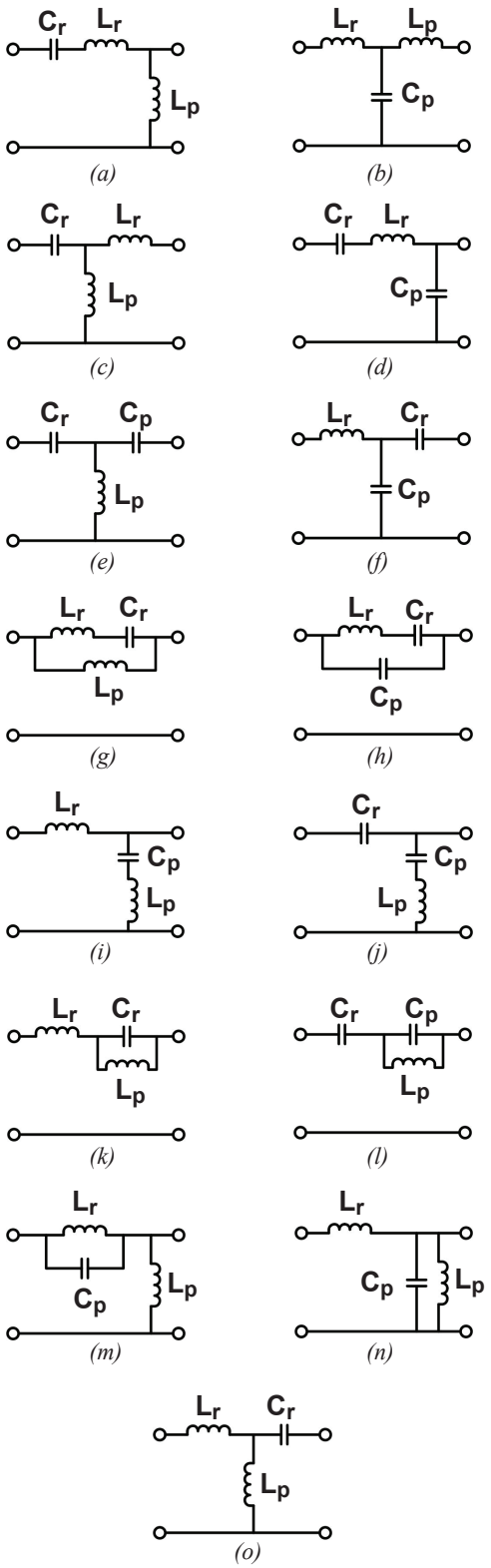

Figure 11 – 3-element resonant tanks work with the voltage source and have all the resonant elements participating in resonance: (a) tank I, (b) tank II, (c) tank III, (d) tank IV, (e) tank V, (f) tank VI, (g) tank VII, (h) tank VIII, (i) tank IX, (j) tank X, (k) tank XI, (l) tank XII, (m) tank XIII, (n) tank XIV and (o) tank XV.

There are thirty-six possible resonant tank combinations of 3-element resonant tanks [5]. If we only consider resonant tanks that work with pulsating voltage sources, twenty-three possible resonant tank combinations are left. And fifteen of the twenty-three possible resonant tanks have all the resonant elements participating in resonance. These fifteen 3-element resonant tanks are shown in Figure 11.

Resonant tank I is the LLC-SRC resonant tank and its input-to-output voltage gain curves are shown in Figure 12(a). Similar voltage gain characteristics can be found in resonant tanks II and III. Resonant tank IV is generally called a "LCC" type resonant tank and its input-to-output voltage gain curves are shown in Figure 12(b).

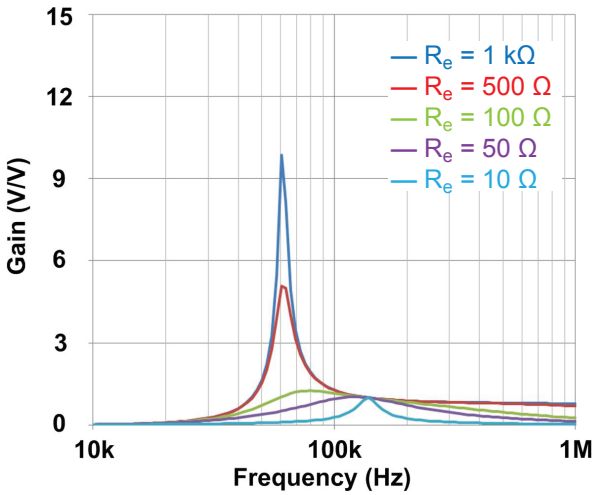

(a)

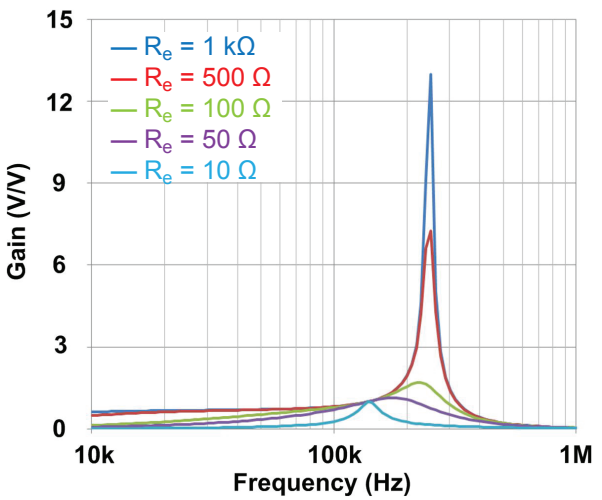

(b)

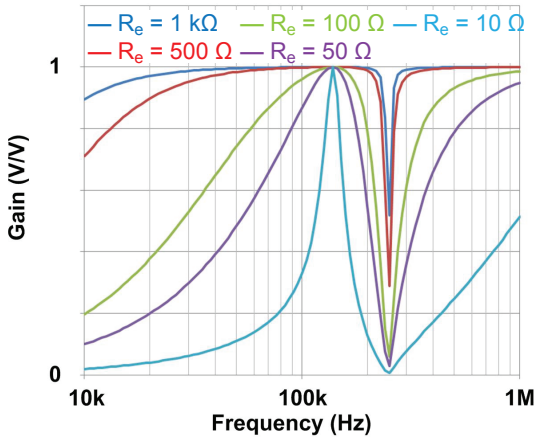

(c)

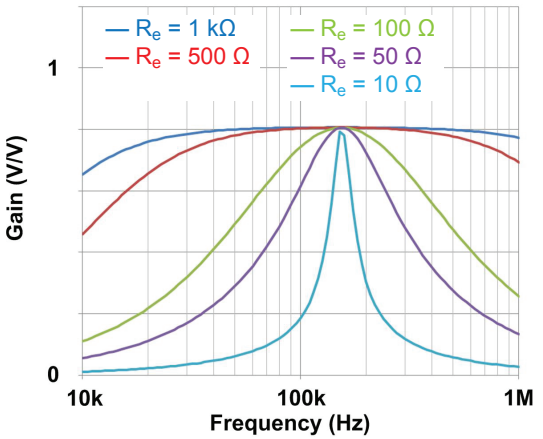

(d)

Figure 12 – Input-to-output voltage gains of: (a) tank I, (b) tank IV, (c) tank VIII and (d) tank XV with C_p=10 nF and L_p=250 µH.

It is notable that the LCC voltage gain peak is higher than the LLC voltage gain peak with the same series parameters C_r=22 nF and L_r= 60 µH. NR can be observed in the gain curves of resonant tanks VII through XIV. The voltage gain of resonant tank VIII is shown in Figure 12(c) as an example. The complicated shape of the gain curves makes the resonant tanks with NR hard to regulate. Resonant tank XV has an inductor divider formed by L_r and L_p which provides lower voltage gain with a SR characteristic, as shown in Figure 12(d).

E. Soft-Switching Criteria

The main benefit of resonant converters is that a resonant converter can achieve soft-switching on its switch network over wide load ranges. Therefore, it is essential to understand the necessary and sufficient conditions of soft-switching or, precisely speaking, zero-voltage switching (ZVS). ZVS means the switch achieves zero voltage before it is turned on. Take a MOSFET (commonly used in switch networks today) as an example. We need a current to completely discharge the MOSFET output capacitor energy before the MOSFET is turned on in order to achieve ZVS. There are three conditions needed to achieve ZVS on MOSFETs in a switch network:

1) Inductive input impedance:

First, we need to ensure a current is present during the turn-on transient to charge or discharge the MOSFET output capacitor, which can be ensured by making the resonant tank inductive in the desired operational frequency range. As shown in Figure 13(a), when the resonant tank is inductive, current is lagging and therefore the switch network output current is greater than zero during the turn-on transient. It is also notable that when a resonant tank is inductive, its impedance curve is a positive slope and its gain curve is a negative slope, as shown in Figure 13(b).

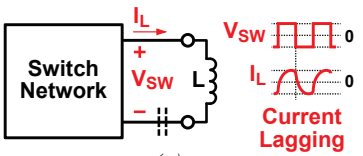

(a)

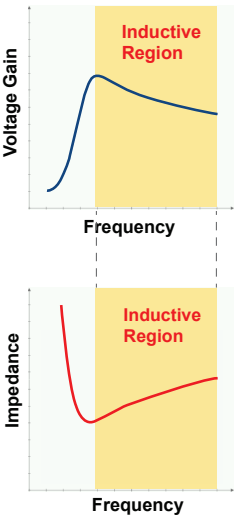

(b)

Figure 13 – Inductive impedance: (a) block diagram and (b) inductive region in gain and impedance curves.

2) Sufficient energy stored in the resonant tank:

Inductive resonant tanks can ensure the MOSFET output capacitors be charged or discharged by the resonant tank current. However, inductor impedance cannot guarantee "zero" voltage switching can be achieved. In addition to the inductor impedance, we need to ensure the energy stored in the resonant tank is larger than the energy stored in the MOSFET output capacitors in the switch network. Let's take the half-bridge LLC-SRC in Figure 14 as an example. The worst-case equation for this LLC-SRC to achieve ZVS is

$$L_m I_{Lm(PEAK)}^2 > C_{OSS} V_{DS(Q1)}^2 \quad (6)$$

where C_{OSS} is the output capacitance of MOSFETs Q_1 and Q_2 and is assumed to be a constant here.

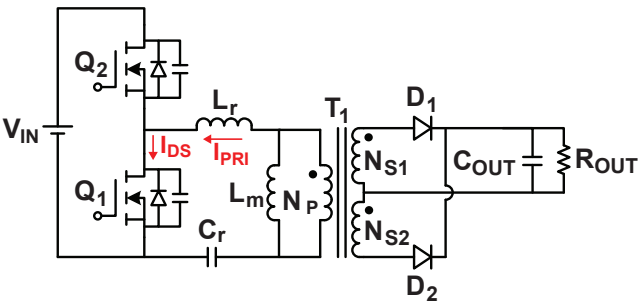

Figure 14 – Half-bridge LLC-SRC.

3) Sufficient dead-time:

The meaning of Equation (6) is that the resonant current is now capable of fully charging or discharging the MOSFET output capacitors. Consider the half-bridge LLC-SRC case shown in Figure 14. If a constant current I_{DS} is used to discharge Q_1 C_{OSS} from the voltage V_{IN} to zero and charge Q_2 C_{OSS} from zero to V_{IN} with the assumption that $C_{OSS(Q1)}$=$C_{OSS(Q2)}$=C_{OSS}, then the time that allows the charge or discharge process to complete can be expressed as

$$t_{d(MIN)} = \frac{2C_{OSS}V_{IN}}{I_{DS}} \quad (7)$$

If the dead-time between Q_1 and Q_2 is less than $t_{d(MIN)}$, ZVS cannot be achieved because the output capacitor charge or discharge process is not completed. The concept is also illustrated in Figure 15. The dead-time (t_2) must be greater than the capacitor discharge time (t_1) to allow a complete discharge process and achieve ZVS.

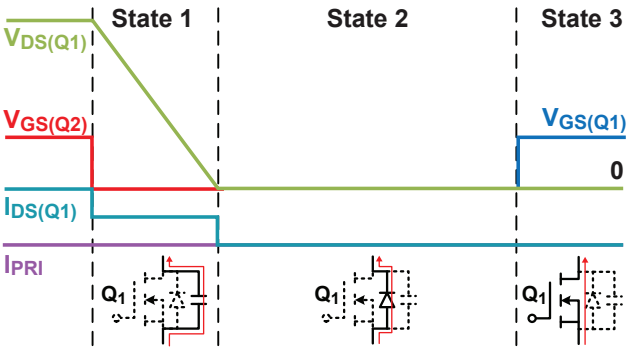

Figure 15 – Switching transient of a half-bridge LLC-SRC.

If all three conditions are met, we can ensure ZVS is achieved on all the MOSFETs inside the switch network.

III. LLC Series Resonant Converter

One common resonant converter application is the isolated DC/DC converter stage after a power factor correction (PFC) circuit in a high efficiency AC/DC power supply, as shown in Figure 16. A PFC circuit boosts the rectified AC input voltage to a well-regulated voltage level, generally around 390 V. Also, a "hold-up time" is generally required in such power supplies to maintain the output voltage regulation while the AC input is interrupted for one to a couple of cycles. To meet the hold-up time requirement, engineers generally design the isolated DC/DC converter to cover as low as a 250 V input voltage.

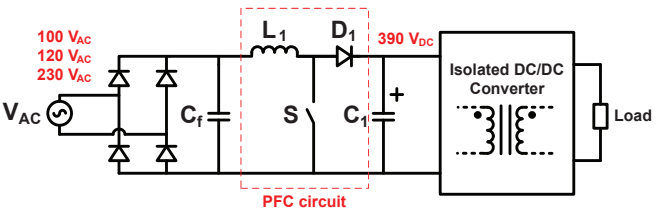

Figure 16 – Switching transient of a half-bridge LLC-SRC.

Resonant converters are good candidates in this application because the soft-switching characteristic enables high converter efficiency. However, it is also important to maintain low circuit costs. In general, half-bridge type switch networks, as shown in Figure 1(b), provide the lowest cost switch network. In addition, if we can

find a resonant tank that can utilize the parameters of the isolation component, i.e. transformer, as a resonant element and work with the half-bridge switch network without adding additional components, we are able to minimize overall circuit cost.

An ideal transformer has its magnetizing inductor in parallel with its input winding, which can be used as the resonant inductor in parallel with the resonant tank output port. Considering 2-element and 3-element resonant tank candidates in Figures 10 and 11, we find that resonant tanks B, H, I, III, V, XIII, XIV and XV are feasible to utilize the transformer magnetizing inductor as one resonant element. However, an additional DC blocking capacitor is required for tanks H, XIII, XIV and XV to work with a half-bridge switch network.

In the real world, a transformer always comes with a leakage inductor in series with the transformer windings. If the series connected leakage inductor can be used as a resonant inductor, we can further reduce the circuit cost. Among the twenty-three 2- and 3-element resonant tank candidates, only tank I can utilize both the transformer leakage inductor and magnetizing inductor as resonant inductors and work with the half-bridge switch network to provide the lowest circuit cost. Resonant converters with tank I are generally called LLC series resonant converters (LLC-SRC). Detailed analysis of an LLC-SRC has already been made in [6]. This section mainly focuses on the LLC-SRC key characteristics and performance.

The LLC-SRC input-to-output voltage gain derived from FHA is expressed as below:

$$\frac{nV_{OUT}}{V_{IN}/2}=\frac{1}{\sqrt{\left(\frac{1}{\omega^2 L_m C_r}\right)^2\left(\frac{\omega^2}{\omega_m^2}-1\right)^2+\left(\frac{1}{\omega C_r n^2 R_{OUT}}\right)^2\left(1-\frac{\omega^2}{\omega_r^2}\right)^2}} \tag{8}$$

where $n=N_p:N_{S1}=N_{S2}$, $\omega_r=2\pi f_r=(L_rC_r)^{-0.5}$ and $\omega_m=2\pi f_m=[(L_r+L_m)C_r]^{-0.5}$. Its gain curves are also illustrated in Figure 12(a). The series resonant elements, L_r and C_r, resonate with the parallel resonant element, L_m, to provide the PR of the LLC-SRC with the resonant frequency, f_m. The series resonant elements resonate by themselves to provide the SR of the LLC-SRC with the resonant frequency, f_r. Therefore, LLC-SRC can either provide a voltage step-up function utilizing the PR characteristic or a voltage step-down function utilizing the SR characteristic.

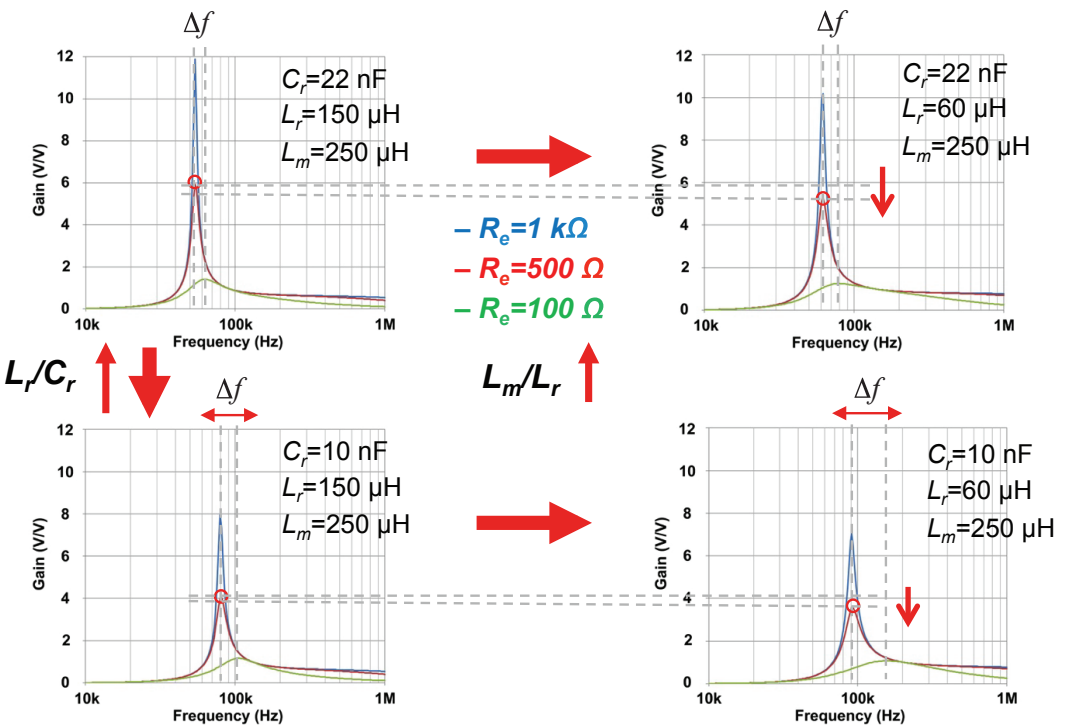

Figure 17 – Effect of LLC-SRC resonant parameter variations.

The effect of resonant parameter variations is illustrated in Figure 17. It is notable that with the increase of the L_m/L_r ratio, the peak value of the gain curve decreases. That is, the voltage regulation range is reduced. With the increase of the L_r/C_r ratio, the difference between the two resonant frequencies increases, which means the operational frequency variation increases. From Figure 17, we know that both the L_m/L_r and L_r/C_r ratio need to be low enough to have wide voltage regulation range and narrow operational frequency variation.

However, the current I_{Lm} is circulating between the switch network and resonant tank at the input side and doesn't transfer to the output side, as can be seen in Figure 18. If L_m is reduced to keep the L_m/L_r ratio low for a wide voltage regulation range, I_{Lm} will increase and therefore reduce the converter efficiency. Hence, a trade-off between the efficiency and voltage regulation range must be made.

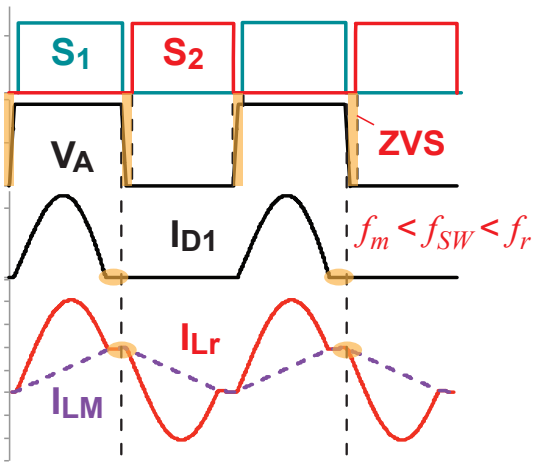

Figure 18 – LLC-SRC key waveforms at $f_m<f_{SW}<f_r$.

Because ZVS is achieved in LLC-SRC, it is possible to push the switching frequency higher to reduce the converter size while still maintaining higher converter efficiency. A 385 V input to 48 V/1 kW output, 1 MHz LLC-SRC design example with gallium-nitride (GaN) FETs is shown in Figure 19(a) along with its key waveforms in 19(b) and efficiency results in 19(c). The power stage volume is 6 in^3 which yields a 167 W/in^3 power density. The minimum power stage dimension not only provides high power density, but also allows a lightweight converter. The weight of this 1 kW design is less than 210 g.

ZVS gives a clean V_{DS} waveform, as can be seen in Figure 19(b), and minimizes the switching losses. Therefore, the efficiency can be maintained at a high level. In this design, a peak 97.6% efficiency is achieved. Other design details can be found in [7].

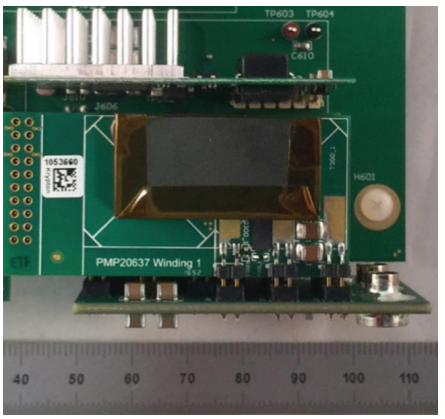

(a)

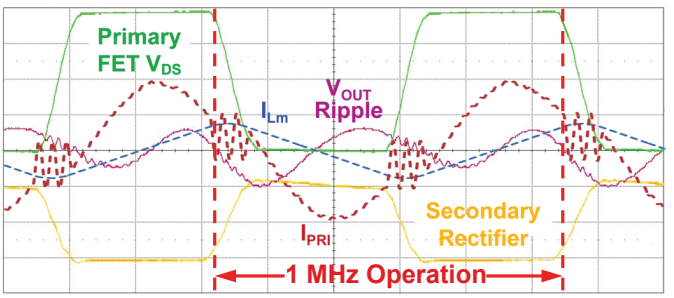

(b)

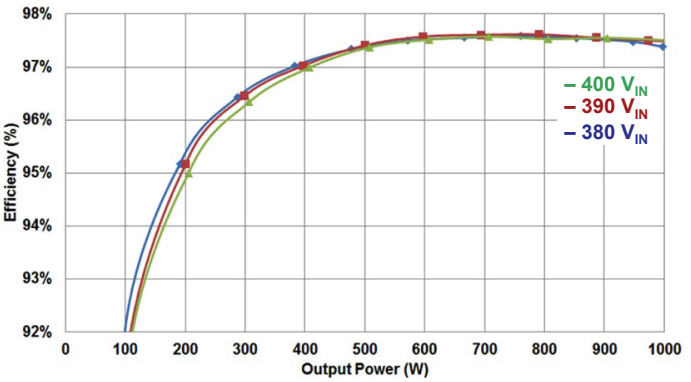

(c)

Figure 19 – 1 MHz LLC-SRC: (a) power stage, (b) key waveforms and (c) efficiency.

IV. Resonant Converters for Wide Input/Output Voltage Ranges

The need for a PFC circuit is generally driven by standards, such as EN61000-3-2 [8], ENERGY STAR® [9] and 80 PLUS® [10]. Low current harmonics are required in EN61000-3-2, as shown in Figure 20, and a high power factor is required in both ENERGY STAR® and 80 PLUS®.

Harmonic Order N	75 W < P < 600 W Maximum Permissible Harmonic Current (mA/W)
3	3.4
5	1.9
7	1.0
9	0.5
11	0.35
13	0.269
15 < n < 39	3.85/n

Figure 20 – EN61000-3-2 harmonic requirements.

The use of a PFC circuit does reduce the reactive power and the demand from the distribution system. However, a PFC circuit also increases the power supply bill of material cost. If the PFC circuit is removed, the input voltage range of the isolated DC/DC converter becomes much wider. An AC/DC power supply example without PFC is shown in Figure 21. With 120 V_{AC} input, the DC voltage after the bridge rectifier varies from 100 V to 200 V, which gives the isolated DC/DC converter a higher $V_{IN(MAX)}/V_{IN(MIN)}$ voltage ratio. In lighting and battery charger applications, a wide output voltage range is also required. If a resonant converter is applied to these types of applications, a high voltage gain resonant converter must be chosen to fulfill the demand of the wide voltage gain range.

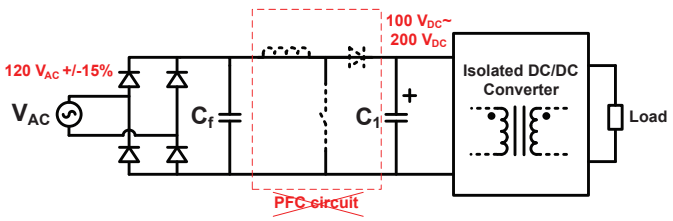

Figure 21 – AC/DC power supply without PFC circuit.

To have high voltage gain, we must select resonant tanks with PR. Tanks B, C, I, II, III, IV, V, VI and XIII in 2- and 3-element resonant converters are the possible candidates. Tank XIII can be ruled out because its NR may lead to a difficult to control design. It is notable that tanks I, II and III have two inductors and one capacitor (2L1C) and tanks IV, V and VI have two capacitors and one inductor (1L2C). Here, we pick tank I from the 2L1C resonant tank candidates and tank IV from the 1L2C candidates for the discussion of wide input or output voltage resonant converter design considerations.

As wide voltage gain variation is needed, the resonant converter must operate in a region that has wide voltage gain variation and narrow frequency variation. In addition, the input impedance must be kept inductive to maintain soft-switching. The desired operating regions of tanks I and IV are shown in Figure 22. Wide voltage gain variation and inductive impedance can only occur between two resonant frequencies in tank I and above the higher resonant frequency in tank IV. It is notable that the voltage gain slope is dominated by the ratio of the two resonant inductors in tank I and the ratio of the resonant inductor and parallel capacitor in tank IV. One interesting difference between these two resonant tanks is that the voltage gain decreases to zero much quicker in tank IV than tank I when the switching frequency goes high. This feature implies that with tank IV, a zero to V_{OUT} (V_{OUT} could be any number greater than zero) voltage regulation range can be achieved simply with FM. Tank I, on the other hand, will require other control methods, such as burst mode control, to realize the zero to V_{OUT} voltage regulation range.

A lighting specification, shown in Table 1, is used here to further understand the difference between tank I and tank IV. A half-bridge LLC-SRC (resonant converter with tank I) and LCC resonant converter (resonant converter with tank IV) shown in Figure 23 are used in the comparison.

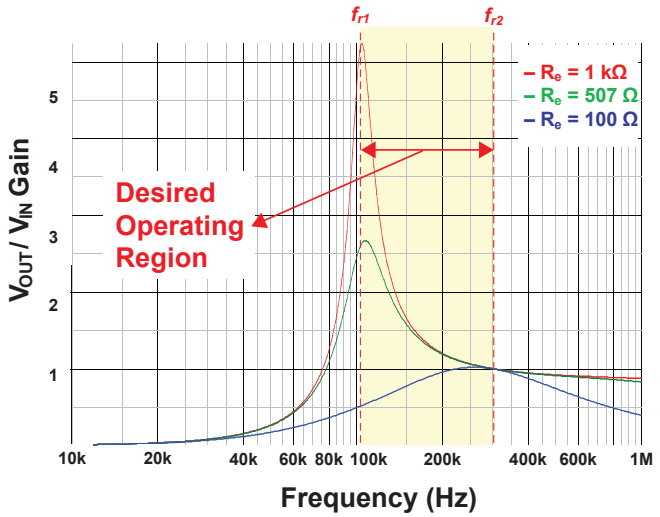

(a)

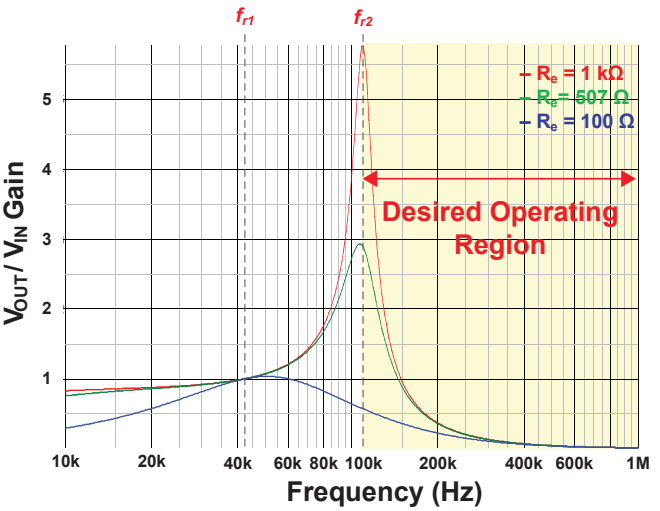

(b)

Figure 22 – Desired operating region for wide input or wide output applications: (a) tank I and (b) tank IV.

Input voltage	400 V to 460 V
Output voltage	100 V to 200 V
Output regulation	Constant voltage at 200 V or constant current at 1A

Table 1 – Lighting specification for tank I and tank IV comparisons.

First, we need to determine the transformer turns ratio to start the designs. Notice that the LLC-SRC has unity voltage gain at the resonant frequency, f_{r2}, as can be seen from Figure 22, and the voltage gain is still close to unity even when the switching frequency is high. Therefore, we

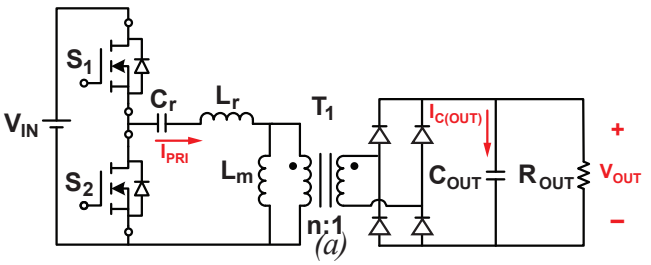

(a)

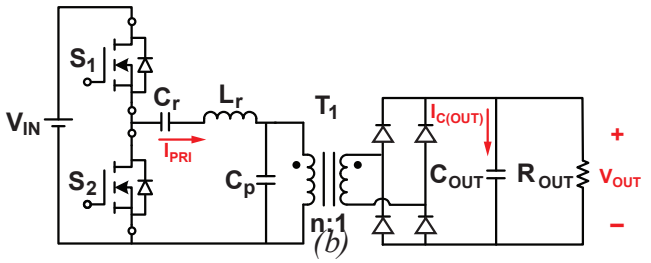

(b)

Figure 23 – LLC-SRC and LCC resonant converter used in the comparison with lighting specification: (a) LLC-SRC and (b) LCC resonant converter.

must set the transformer turns ratio of the LLC-SRC to allow a unity voltage gain on the resonant tank at the maximum input voltage and minimum output voltage to minimize the operational frequency variation range. That is,

$$n = \frac{V_{IN(MAX)}}{2} \frac{1}{V_{OUT(MIN)}} \tag{9}$$

Using the specification in Table 1, n can be calculated to be 2.3 for LLC-SRC. As the LCC resonant converter has a much wider operating range than the LLC-SRC, we only need to ensure that the LCC resonant converter has a high enough voltage gain with minimum input voltage and maximum output voltage at a full load. A unified transformer turns ratio n=2.5 is selected for both the LLC-SRC and LCC resonant converters in order to provide a fair comparison and ease the transformer design.

Second, we need to decide on the operation point for both designs. To make a fair comparison, we design both converters to have the same 130 kHz switching frequency at 400 V_{IN} and 200 V/1 A output. Once the operating point is set, we can then design both converters to ensure the voltage gain is high enough to cover the full input and output

ranges with minimum circulating current, i.e. by maximizing the impedance of the parallel resonant elements: L_m and C_p. The following parameters are selected for comparison:

LLC-SRC:

- L_r = 40 µH, L_m = 300 µH, C_r = 7 nF

LCC resonant converter:

- L_r = 300 µH, C_r = 0.047 µF, C_p = 8.2 nF

Figure 24 shows the LLC-SRC and LCC resonant converter gain curves with the above parameters. The corner operating points, 400 V_{IN}/200 V_{OUT} and 460 V_{IN}/100 V_{OUT}, are highlighted in Figure 24. Using Equation (5), the equivalent load resistance (R_e) can be calculated to be 1 kΩ and 507 Ω with 100 V/1 A and 200 V/1 A output, respectively. Both converters have the same operating point at 130 kHz with 400 V_{IN} and 200 V/1 A output. While with 460 V_{IN}, the LLC-SRC operating point goes to 250 kHz and the LCC resonant converter is still below 150 kHz. That is, if the input or output regulation range is wider than the specifications listed in Table 1, LLC-SRC (or other 2L1C resonant converters) may no longer be feasible because of the wide frequency variation range. Instead, 1L2C converters, like a LCC resonant converter, will be better candidates in such applications in terms of high voltage gain.

However, if we look at the key current waveforms in the two converters used in the comparison, higher RMS current is observed in the resonant tank and output of the LCC resonant converter – as can be seen from the simulation results in Table 2 below. Higher RMS current implies lower converter efficiency. Hence, a LCC resonant converter in general will have lower efficiency than a LLC-SRC. Therefore, a trade-off between the voltage regulation range and efficiency must be made during the topology selection process.

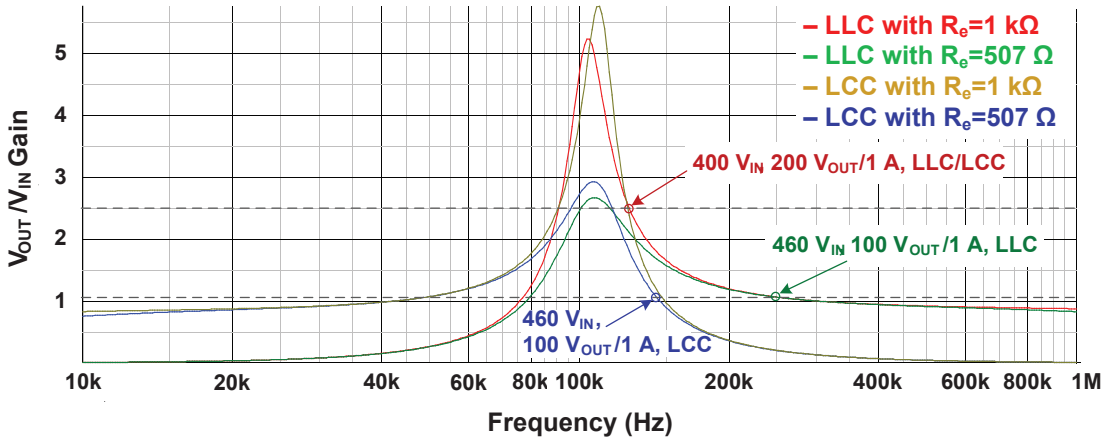

Figure 24 – LLC-SRC and LCC resonant converter gain curves used in the comparison.

V_{IN} (V)	V_{OUT} (V)	I_{OUT} (A)	LLC I_{PRI} (A_{RMS})	LCC I_{PRI} (A_{RMS})	LLC f_{SW} (kHz)	LCC f_{SW} (kHz)	LLC $I_{C(OUT)}$ (A_{RMS})	LCC $I_{C(OUT)}$ (A_{RMS})
400	200	1	1.73	2.69	131	122	1.37	1.97
460	200	1	1.69	2.76	138	125	1.32	1.98
400	100	1	0.775	1.65	196	130	0.904	1.66
460	100	1	0.709	1.7	245	135	0.722	1.67

Table 2 – Simulation results of the corner conditions of the LLC-SRC and LCC resonant converters.

V. Resonant Converter Variations

From Section II to IV, we have gone through the resonant converter fundamentals, designs and applications based on conventional resonant converter structure as shown in Figure 1(a). However, it is not necessary to have an explicit resonant tank and rectifier stage. Instead, it is possible to have components inside the rectifier stage participating in resonance. Take the 3-element resonant tank III and its rectifier network as an example. It is possible to have the resonant inductor, L_{r1}, be placed at the rectifier network after the rectifier diodes, as shown in Figure 25.

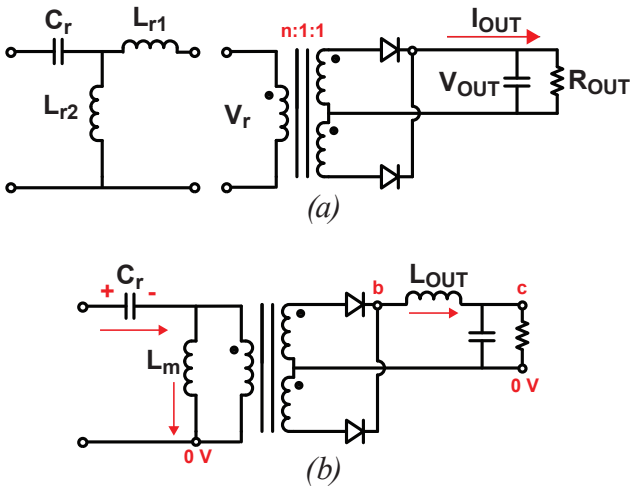

Figure 25 – (a) 3-element resonant tank III and its output network and (b) proposed CLL resonant converter with implicit resonant tank and output network.

The benefits of having a resonant inductor placed after the rectifier are possibly lower power losses and a size reduction in the inductor. First, L_{r1} is equivalent to n^2L_{OUT} so for resonant frequencies

$$f_{r1} = \frac{1}{2\pi\sqrt{C_r(L_{r1}//L_{r2})}} = \frac{1}{2\pi\sqrt{C_r(n^2L_{OUT}//L_{r2})}}$$

$$f_{r2} = \frac{1}{2\pi\sqrt{C_rL_{r2}}} \qquad (10)$$

In a voltage step-down application, n is greater than one and therefore $L_{OUT}<<L_{r1}$. So, L_{OUT} can be much smaller than L_{r1} in inductance. If we look at the input current, I_{Cr}, and the inductor current, $I_{L_{OUT}}$, in Figure 26 we find that the resonant inductor current $I_{L_{OUT}}$ is no longer swinging from positive to negative like I_{Cr}. Instead, $I_{L_{OUT}}$ stays non-zero. This implies the B-H hysteresis of $I_{L_{OUT}}$ stays in the 1st quadrant instead of across all 4 quadrants, as the resonant inductors in the original tank III. That is, the core loss of L_{OUT} will likely be less than the core loss of L_{r1} in the original tank III. Especially at $f_{SW}>f_{r1}$, $I_{L_{OUT}}$ goes into continuous conduction mode (CCM) with less current ripple, which means the B-H hysteresis area is further reduced as well as core losses. Therefore, efficiency can be further improved when the switching frequency is higher. Also, inductor size of L_{OUT} could be smaller than L_{r1} because of a smaller B-H hysteresis area.

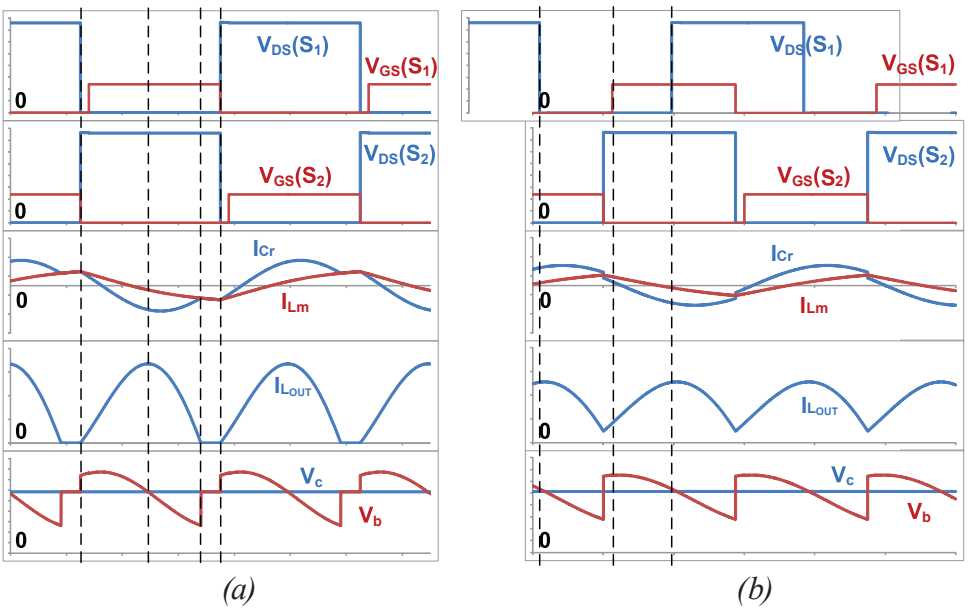

Figure 26 – CLL resonant converter key waveforms: (a) $f_{SW}<f_{r1}$ and (b) $f_{SW}>f_{r1}$.

250 W LLC-SRC and CLL resonant converter prototypes were built to verify the statements above. The two prototypes have the same 370 µH parallel inductor (L_m), 33 nF resonant capacitor, and n=8 turns ratio. The only difference between the two prototypes is that different resonant inductors are applied. In LLC-SRC, the resonant inductor (L_r) has 72 µH inductance. In the CLL resonant converter, the resonant inductor (L_{OUT}) has 1 µH inductance. The actual inductors used are shown in Figure 27, an 11.4 mm x 12.1 mm x 9.5 mm inductor was used for the CLL resonant inductor and an inductor with Litz wire and an EE19 core was used for the LLC-SRC inductor. Notice that the resonant inductor with the EE19 core is 5 times larger than the CLL resonant inductor in volume. Finite element analysis (FEA) was made to both resonant inductors with the EE19 core with 3C95 material and a copper sheet with 10 mm width and 0.05 mm thickness for analysis simplicity. The key parameters used in the FEA are shown in Table 3. The inductance of the two resonant inductors is equivalent in the linearized circuit by taking the turns ratio into account, i.e. $L_r=n^2L_{OUT}$. Simulation results are shown in Table 4. As can be observed in Table 4, the total resonant inductor losses are greatly reduced when the switching frequency is higher than the resonant frequency ($f_{SW}>f_{r1}$).

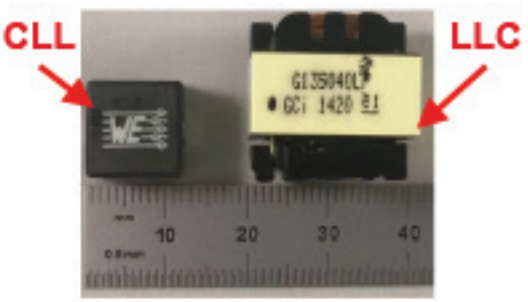

Figure 27 – Resonant inductors used in CLL resonant converter and LLC-SRC.

	LLC	CLL
Inductance	73 µH	1.2 µH
Turns	24	3
Parallel winding	1	8
R_{DC}	31.5 mΩ	0.48 mΩ

Table 3 – Resonant inductor parameters used in FEA.

	$f_{SW} = f_{r1}$	$f_{SW} > f_{r1}$	$f_{SW} < f_{r1}$
LLC L_r loss (winding/ core)	0.87 W (0.4 W/0.47 W)	1.11 W (0.38 W/ 0.73 W)	0.69 W (0.35 W/ 0.34 W)
CLL L_r loss (winding/ core)	0.43 W (0.12 W/ 0.31 W)	0.23 W (0.07 W/ 0.15 W)	0.53 W (0.14 W/ 0.39 W)

Table 4 – Loss analysis results in FEA.

Efficiency measurements were made with the output voltage regulated to 27.5 V on both prototypes. The measurement results are shown in Figure 28. The LLC-SRC efficiencies are nearly independent from the given input voltages with a 94.7% peak efficiency. On the other hand, the CLL resonant converter efficiencies vary with the input voltage. When the input voltage and switching frequency are higher than the resonant frequency ($f_{SW}>f_{r1}$), the CLL resonant converter yields a better efficiency than the LLC-SRC. 95.7% peak efficiency is achieved with a 430 V input voltage. Detailed analysis and design details can be found in [11][12].

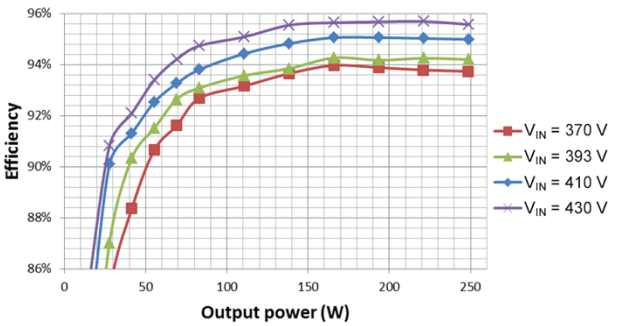

(a)

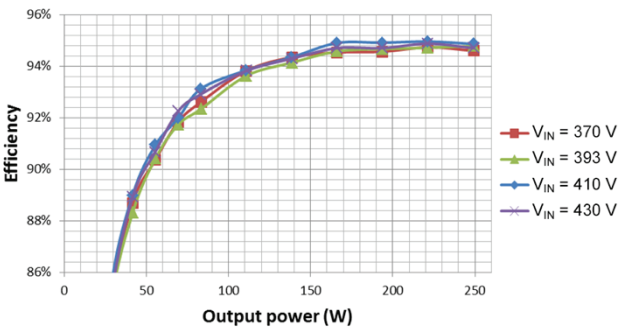

(b)

Figure 28 – Converter efficiency with 27.5 V output and different input voltages: (a) CLL resonant converter and (b) LLC-SRC.

VI. Resonant Converter Design Challenges and the Effects of Real Life Parasitics and Parameters

Although FHA helps us to better understand resonant converter gain characteristics, there are still some details a designer should always keep in mind, especially the operational states, transient response and effects of component parasitics.

A. Operational States

The operational states of resonant converters are very different from PWM converters. Unlike PWM converters, there are more than two operational states – discontinuous conduction mode (DCM) and CCM. For example, five possible operational states of a LLC-SRC across different switching frequencies and load conditions are shown in Figure 29. Unlike PWM converters, the output rectifier current, I_{D1} in Figure 29, is not always non-zero after an input switch is turned off. In addition, the rectifier turn-off timing is not only load dependent but also frequency dependent. As depicted in [13], voltage type self-driven synchronous rectifiers cannot be applied to the resonant converters with pulsating voltage present at the rectifier network input. Instead, turning the synchronous rectifier on and off by detecting the rectifier voltage – V_{DS} sensing technique – is more promising for a resonant converter with a synchronous rectifier.

B. Transient Response

Unlike PWM converters, the state-space average method [14] is no longer suitable for a resonant converter to obtain an accurate small signal model for a transient response analysis. This is because the DC component of the state variables in the state-space average method needs to be dominant for the model to be accurate and some state variables in a resonant converter do not have a DC component. In addition, the natural resonant frequencies of the resonant tank strongly interact with the switching frequency as they are generally close to each other. This situation generally results in a double pole in its plant transfer function [15].

Traditionally, variable frequency control (VFC) – or so called "FM" – is applied to a resonant converter. A block diagram of an LLC-SRC with VFC is shown in Figure 30. The sensed output voltage signal is compensated and transferred through a compensation network and the opto-coupler is then fed into a voltage controlled oscillator (VCO) to generate the driving signals at the desired frequency. Since only the output voltage signal is used to process the error in the system, the double pole in the plant transfer function remains intact. Due to the presence of a double pole in the plant transfer function, it is more complex to stabilize the loop and obtain a very good transient response. Therefore, the VFC is analogous to voltage mode control for PWM

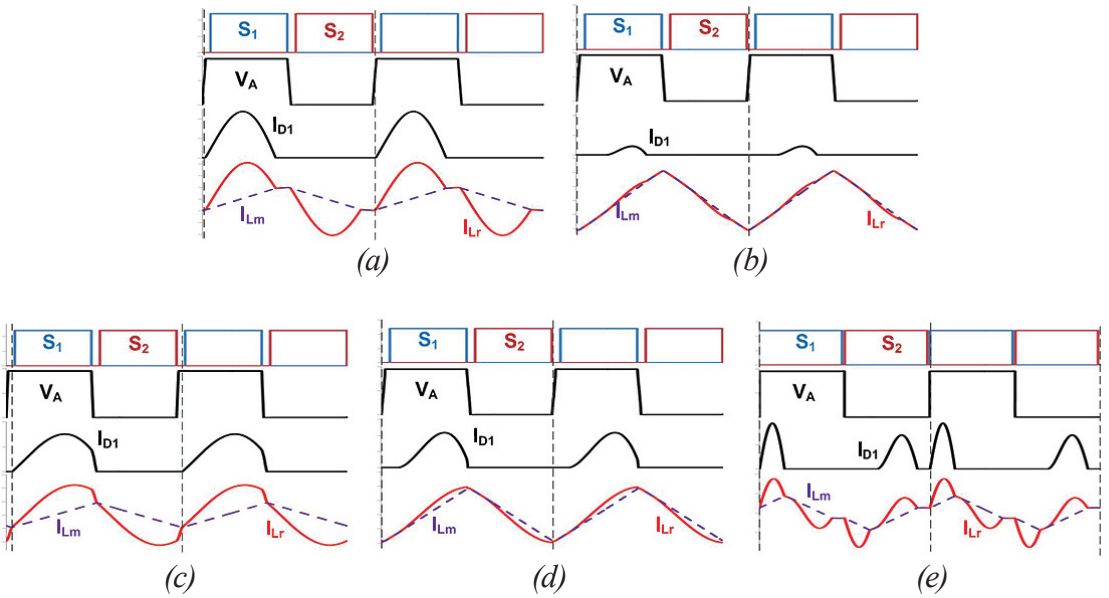

Figure 29 – Possible LLC-SRC operational states.

converters. In general, resonant converters with VFC have a slow transient response and higher order plant transfer function. And because no signals from the input side are taken, the input voltage rejection is also poor. To have better transient response of a VFC resonant converter, a type III compensator along with a better opto-coupler is generally required.

Another significant challenge in using the VFC is optimizing the performance of the converter at light load – specifically, it is challenging to implement some form of burst mode and obtain very good standby power performance along with a good transient response out of burst mode operation. As burst mode periodically switches between the idle state and high power state, it is difficult to optimize the burst mode operation to give good efficiency, transient response and audibility performance, especially with VFC.

Current mode control for resonant converters has recently been introduced in the field to address light load performance and transient response issues. For example, the hybrid hysteresis control (HHC) proposed in TI UCC256301 [16] utilizes a current signal from a resonant capacitor in the resonant tank. The block diagram of an LLC-SRC with HHC is shown in Figure 31. The resonant capacitor current signal is extracted from a capacitor divider and fed into the controller together with the compensated voltage signal. With the current information at the input side, the HHC is analogous to current mode control. In general, a fast transient response can be expected and the system should be much easier to stabilize.

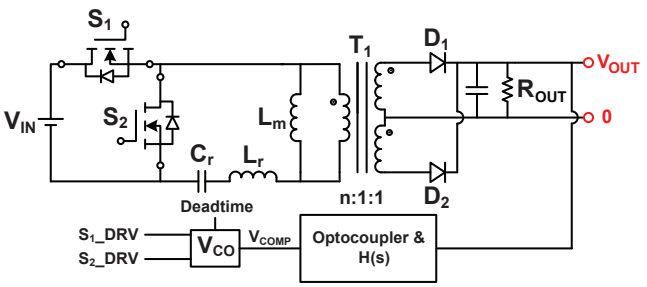

Figure 30 – Block diagram of LLC-SRC with VFC.

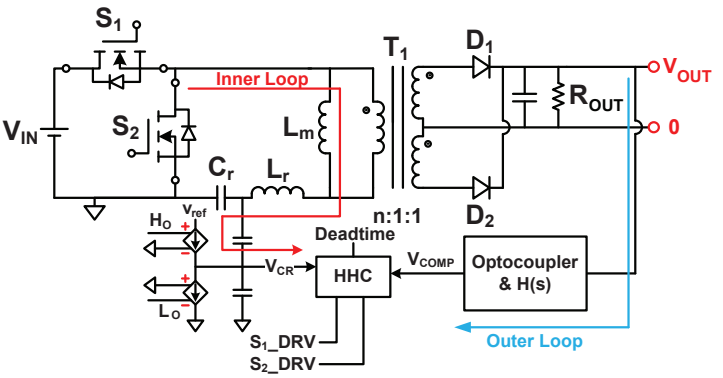

Figure 31 – Block diagram of LLC-SRC with HHC.

Figure 32 shows the frequency response plot on the same power stage with either VFC or HHC. A 1st order system can be observed on the plant gain with HHC, which makes the compensation network design easier. Also, it is much easier to get a faster transient response. Load transients from no load to full load with both VFC and HHC are also taken and shown in Figure 33. Larger than 20% V_{OUT} deviation is observed on the LLC-SRC with VFC, while there is only 1.25% V_{OUT} deviation on the LLC-SRC with HHC. In a HHC control scheme, since it has a fair idea of the tank current, it is possible to have a better control of the energy and the calculation of the optimal efficiency for a burst packet. This makes the trade-off between the transient response, light load efficiency and audible noise much simpler to make.

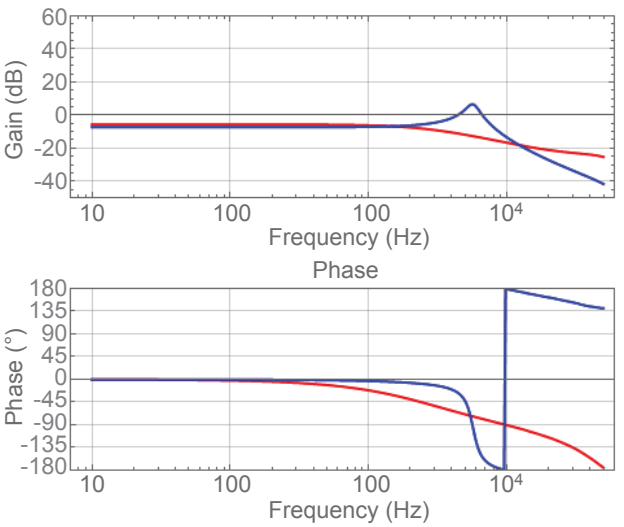

Figure 32 – LLC-SRC plant frequency responses.

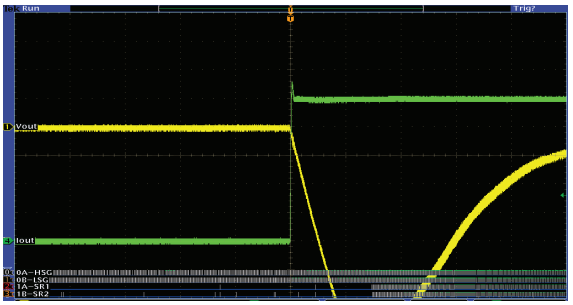

(a)

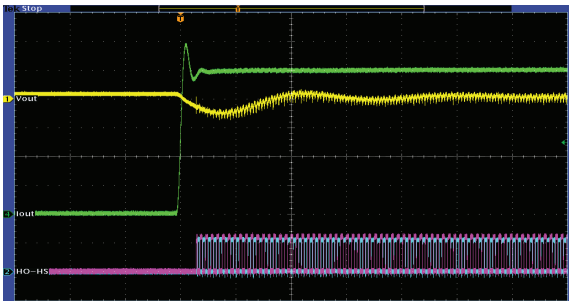

(b)

Figure 33 – LLC-SRC load transient responses with (a) VFC and (b) HHC.

C. Component Parasitics

Transformers are usually used in a resonant converter rectifier network to provide galvanic isolation. Ideally, the transformer can be modeled as windings with infinite inductance, such as the LCC resonant converter used in Section IV. However, the magnetic inductance of a real transformer is a finite number. In addition, the windings of a real transformer will not be perfectly coupled. That is, leakage inductance will be present in a transformer. If we consider the LCC resonant converter with the parameters used in Section IV and a real transformer model with L_k=15 µH and L_m=500 µH shown in Figure 34, the voltage gain curve will change from Figure 35(a) to (b) because both L_k and L_m participate in the resonance. As can be observed from Figure 35, the inductors from the transformer can alter the operation point significantly. Therefore, transformer inductance must be taken into consideration when designing a resonant converter.

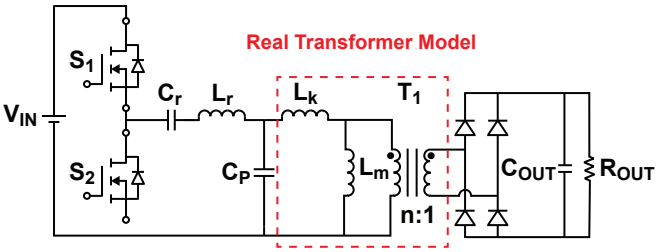

Figure 34 – LCC resonant converter with leakage and magnetizing inductors modeled in the transformer.

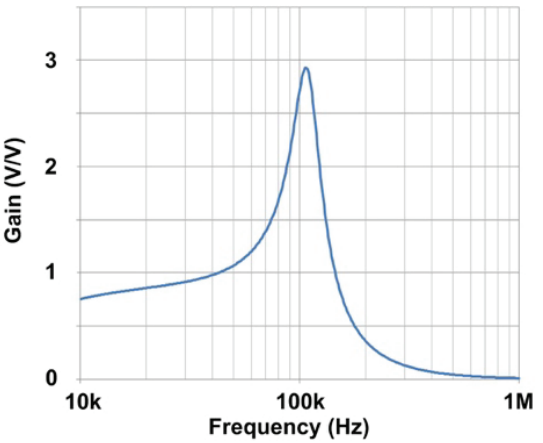

(a)

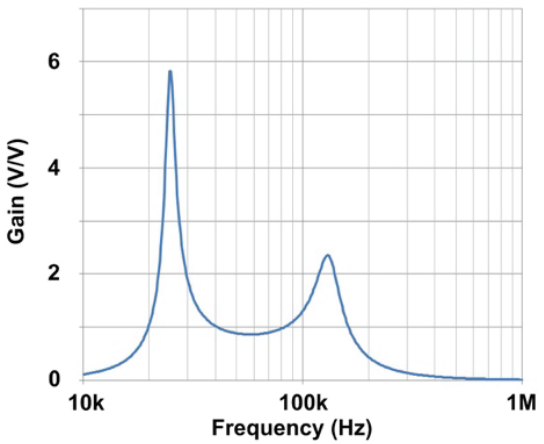

(b)

Figure 35 – LCC voltage gain with R_e=507 Ω and (a) ideal transformer model and (b) real transformer model.

Other than transformer inductance, transformer winding parasitic capacitance, C_{TX}, also affects the resonant converter operation, especially during the dead-time period. The circuit in Figure 36 is the half-bridge LLC-SRC (Figure 14) circuit

model at dead-time considering C_{TX}, where I_{Lm} is assumed to be a constant ($C_{OUT(tr)}$ is the MOSFET output capacitance). If C_{TX} is negligible, I_{Lm} will be fully used to charge or discharge the output capacitors of the MOSFETs. With the presence of C_{TX}, partial I_{Lm} is now going to discharge C_{TX} and leads to a current dip on I_{Lr} during the dead-time, as shown in Figure 37. Because of the current reduction, the $C_{OUT(tr)}$ charge or discharge time is longer and may require longer dead-time. Even worst, we could lose soft-switching if C_{TX} is too large. Longer dead-time means the effective conduction time reduces and results in a higher current RMS and lower converter efficiency. Therefore, it is very important to keep the transformer parasitic capacitance low [17].

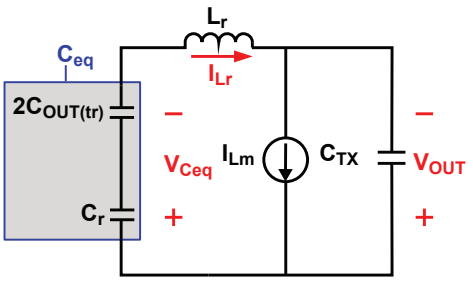

Figure 36 – Equivalent resonant circuit during dead-time.

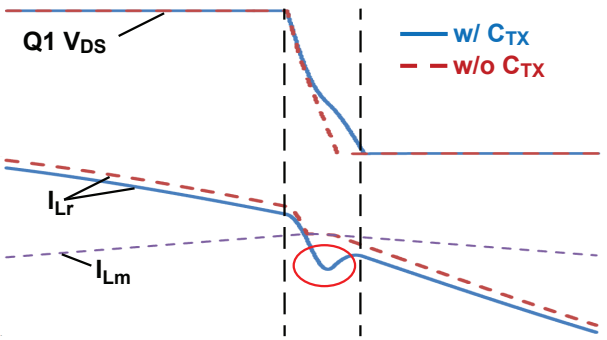

Figure 37 – Effect of transformer parasitic capacitor during dead-time period.

If a resonant converter has high resonant frequencies, ringing or oscillation could be observed due to lower resonant tank inductance and capacitance values. Take the 1 MHz LLC-SRC design used in Section III as an example. Ringing is found during dead-time period, as shown in Figure 38. The high frequency ringing can cause additional loss and electromagnetic interference problems. The 1 MHz LLC-SRC prototype power stage, shown in Figure 39, is modeled as the circuit shown in Figure 40, where $C_{OUT(Q)}$ is the input GaN FET output capacitance, C_P is the parasitic capacitance of the input winding, L_p is the leakage inductance (i.e., L_r) of the input winding, L_s is the "reflected" leakage inductance of the secondary windings, C_{PS} is the inter-winding capacitance, $C_{OUT(SR\_eq)}$ is the "reflected" output capacitance of the synchronous rectifier GaN FETs SR_1 and SR_2 and C_s is the "reflected" secondary winding capacitance. According to the dead-time circuit model, the equivalent capacitance that the current I_{Lm} needs to charge or discharge can be found to be

$$C_{eq} = 2C_{PS} + \frac{1}{\frac{1}{2C_{OUT(SR\_eq)} + C_S} + \frac{1}{2C_{OUT(Q)} + C_P}} \quad (11)$$

It is found that both the winding capacitance and GaN FET output capacitance dominate the C_{eq}. Therefore, it is essential to minimize both winding capacitance and GaN FET output capacitance for better performance.

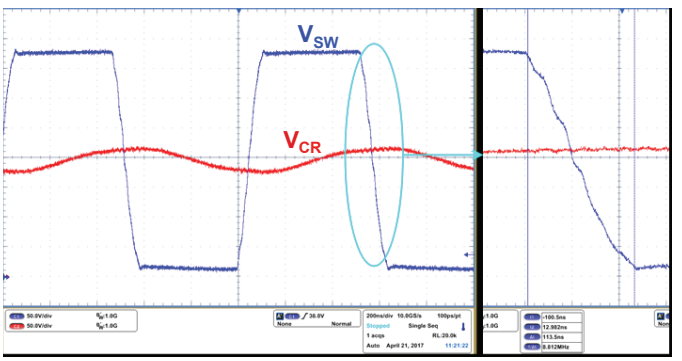

Figure 38 – 1 MHz LLC-SRC prototype switching waveform.

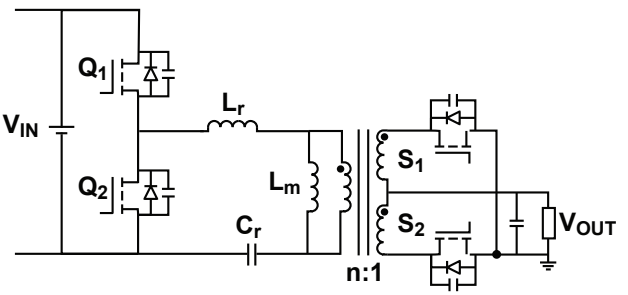

Figure 39 – Schematic of the 1 MHz LLC-SRC prototype power stage.

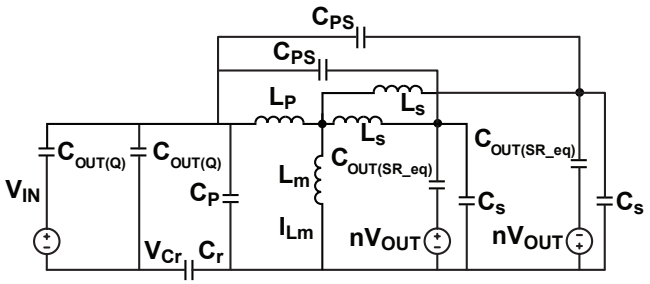

Figure 40 – 1 MHz LLC-SRC power stage model during dead-time.

Besides transformer parasitics and the MOSFET's output capacitance, another key factor that can affect a resonant converter performance is the MOSFET body diode in the switch network. As depicted in Figure 15, there is always a period during the dead-time that the body diode conducts current. When the body diode conducts current, a reverse current is required to remove the reverse recovery charge, Q_{rr}, as shown in Figure 41. During the startup transient of a resonant converter, it is possible that the reverse diode current did not occur and leads to a body diode incomplete reverse recovery. The incomplete reverse recovery issue is illustrated in Figure 42. In the first half-period, high current flows through the resonant tank because the zero output voltage leads to a short (or partial short) circuit of some resonant elements in the resonant tank. In the following half-period, the current did not resonant to a negative value, therefore the Q_{rr} is not removed. The presence of the Q_{rr} leads to hard switching in the next switching period and results in high voltage stress. This issue can cause component failure due to over voltage stress.

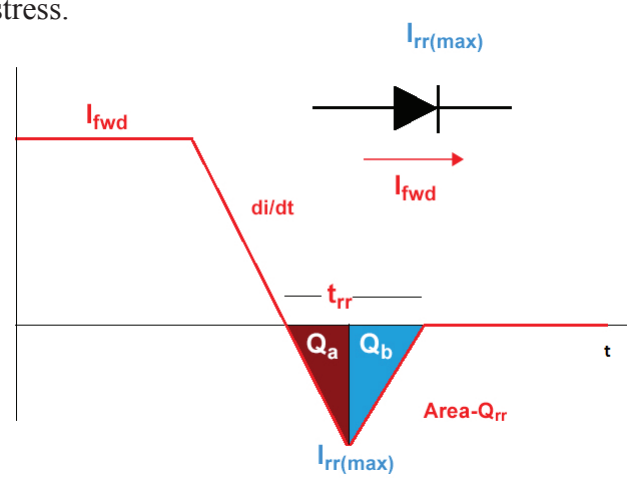

Figure 41 – Diode reverse recovery transient.

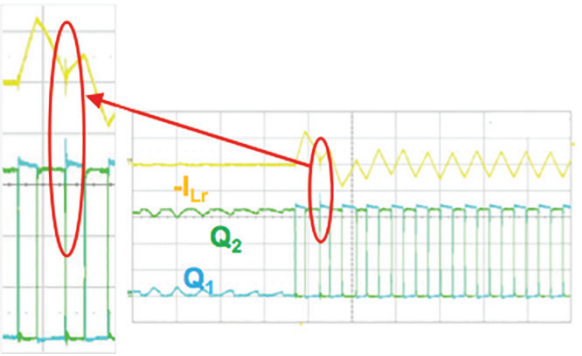

Figure 42 – Incomplete reverse recovery during startup transient.

To ease the concern of the incomplete reverse recovery issue, we need to minimize the body diode conduction duration and to slow down the MOSFET turn-on speed to reduce the body diode reverse recovery current. Or we can simply apply wide bandgap devices like silicon carbide (SiC) or GaN FET as input switches because the wide bandgap devices provide zero or minimum reverse recovery charge [17].

Using a wide bandgap device not only helps on the reverse recovery issue, but also helps to reduce the required dead-time due to smaller output capacitance. An output capacitance comparison between the TI GaN device LMG3410 [18] and a super junction MOSFET with the same level of $R_{DS(ON)}$ is shown in Figure 43. It is observed that the GaN device has more linear output capacitance over the voltage then the super junction MOSFET. As the actual C_{OSS} varies with the drain to source voltage, Equation (7) can be rewritten as

$$t_{D(MIN)} = \frac{2\int_0^{V_{DS}} C_{OSS}(V_{DS})\,dV_{DS}}{I_{DS}} \tag{12}$$

That is, the area under each C_{OSS} curve from 0 V to the maximum operational voltage determines the required dead-time. As can be seen in Figure 43, the GaN device has a much smaller area than the super junction MOSFET. Therefore, less dead-time is required for the GaN device.

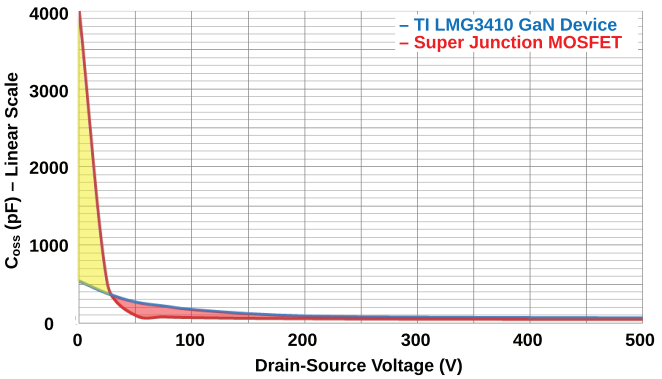

Figure 43 – Output capacitance vs voltage of TI GaN device and a super junction MOSFET.

VII. Summary

This paper has walked through resonant converter fundamentals, resonant topologies for various applications and design considerations. Three fundamental resonances can be found inside resonant tanks: SR, PR and NR. Among the three resonances, PR provides a voltage step-up characteristic and can be found in almost every isolated resonant converter. It is notable that the voltage gain peak increases with the increase of the number of resonant capacitors involved in a PR. NR should be avoided because it limits the frequency range of an inductive impedance resonant tank.

LLC-SRC and LCC resonant converters are further analyzed and applied to different applications. LLC-SRC demonstrates its high efficiency and high density at high frequency operation. LCC resonant converters show less frequency dependence while varying the input or output voltages and higher voltage gain than LLC-SRC. However, higher circulation current in LCC resonant converters may lead to lower converter efficiency.

A new resonant converter structure is proposed with an implicit resonant tank and rectifier network. A CLL resonant converter with the new resonant converter structure demonstrates its advantages in size and efficiency. Table 5 highlights the five resonant converters discussed in this paper. Among them, the LCC resonant converter has the narrowest frequency variation when varying the input or output voltage level but its current stresses are high. In addition to ZVS on the switch network, it is notable that both LLC-SRC and CLL resonant converters can achieve zero current switching (ZCS) on the rectifier network. Different characteristics of each resonant converter give each one a different suitable application. Therefore, it is essential to understand resonant converter fundamentals and key design considerations as depicted in this paper.

	LC Series	*LC Parallel*	*LLC*	*LCC*	*CLL*
	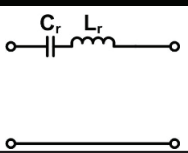	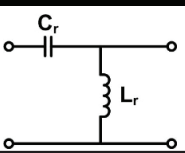	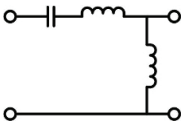	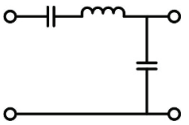	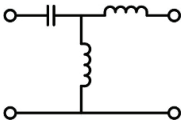
Frequency variation	Wide	Wide	Moderate	Narrow	Moderate
Component voltage/current stresses	Lowest	High	Low	Highest	High
ZVS(input)/ ZCS(output)	ZVS	ZVS	ZVS & ZCS	ZVS	ZVS & ZCS

Table 5 – Comparison of resonant topologies addressed in this paper.

VIII. REFERENCES

[1] Yang, B.; Lee, F. C.; Zhang, A. J. and Huang, G., "LLC resonant converter for front end DC/DC conversion," Proc. APEC, pp. 1108-1112, 2002.

[2] Yu, S. Y. and Kwasinski, A., "Realization and comparison of a new push-pull direct-connected multiple-input converter family for distributed generation applications," Proc. INTELEC, pp. 1-8, 2011.

[3] McDonald, B. and Wang, F., "LLC performance enhancements with frequency and phase shift modulation control," Proc. APEC, pp. 2036-2040, 2014.

[4] Huang, D.; Lee, F. C. and Fu, D., "Classification and selection methodology for multi-element resonant converters," Proc. APEC, pp. 558-565, 2011.

[5] Yang, B., "Topology Investigation for Front End DC/DC Power Conversion for Distributed Power System," Dissertation, Virginia Tech, Blacksburg, VA, 2003.

[6] Huang, H., "Designing an LLC Resonant Half-Bridge Power Converter," Power Supply Design Seminar, 2010.

[7] Texas Instruments, "PMP20637 High Efficiency and High Power Density 1kW Resonant Converter Reference Design with TI HV GaN FET," http://www.ti.com/tool/PMP20637.

[8] Electromagnetic compatibility testing in EMC lab EN 61000−3−2, http://www.rfemcdevelopment.eu/index.php/en/emc-emi-standards/en-61000-3-2-2006-a1-a2.

[9] ENERGY STAR®, "Program Requirements for Single Voltage External AC-DC and AC-AC Power Supplies," https://www.energystar.gov/ia/partners/prod_development/revisions/downloads/FinalSpecV2.pdf?8fd5-1967.

[10] Escova, Inc., "80 PLUS® Certified Power Supplies and Manufacturers," https://www.plugloadsolutions.com/80PlusPowerSupplies.aspx.

[11] Yu, S., "A new compact and high efficiency resonant converter," Proc. APEC, pp. 2511-2517, 2016.

[12] Texas Instruments "PMP9750 400VDC Input to 28V/9A Output Compact, High Efficiency CLL Resonant Converter Reference Design," http://www.ti.com/tool/PMP9750.

[13] Fu, D.; Liu, Y.; Lee, F. C. and Xu, M., "A Novel Driving Scheme for Synchronous Rectifiers in LLC Resonant Converters," IEEE Transactions on Power Electronics, Vol. 24, pp. 1321-1329, 2009.

[14] Middlebrook, R. D., "Small-signal modeling of pulse-width modulated switched-mode power converters," Proceedings of the IEEE, Vol. 76, No. 4, pp. 343-354, April 1988.

[15] Tian, S.; Lee, F. C. and Li, Q., "Equivalent circuit modeling of LLC resonant converter," Proc. APEC, pp. 1608-1615, 2016.

[16] Texas Instruments, "UCC256301 Wide Vin LLC Resonant Controller With High-Voltage Start Up Enabling Ultra-Low Standby Power," http://www.ti.com/product/UCC256301.

[17] Y. S., "Performance evaluation of direct drive high voltage Gallium-Nitride devices in LLC series resonant converters," Proc. WiPDA, pp. 64-69, 2016.

[18] Texas Instruments, "LMG3410 600-V 12-A Single Channel GaN Power Stage," http://www.ti.com/product/LMG3410.

TI Worldwide Technical Support

TI Support

Thank you for your business. Find the answer to your support need or get in touch with our support center at

www.ti.com/support

China: http://www.ti.com.cn/guidedsupport/cn/docs/supporthome.tsp

Japan: http://www.tij.co.jp/guidedsupport/jp/docs/supporthome.tsp

Technical support forums

Search through millions of technical questions and answers at TI's E2E™ Community (engineer-to-engineer) at

e2e.ti.com

China: http://www.deyisupport.com/

Japan: http://e2e.ti.com/group/jp/

TI Training

From technology fundamentals to advanced implementation, we offer on-demand and live training to help bring your next-generation designs to life. Get started now at

training.ti.com

China: http://www.ti.com.cn/general/cn/docs/gencontent.tsp?contentId=71968

Japan: https://training.ti.com/jp

IMPORTANT NOTICE FOR TI DESIGN INFORMATION AND RESOURCES

Texas Instruments Incorporated ('TI") technical, application or other design advice, services or information, including, but not limited to, reference designs and materials relating to evaluation modules, (collectively, "TI Resources") are intended to assist designers who are developing applications that incorporate TI products; by downloading, accessing or using any particular TI Resource in any way, you (individually or, if you are acting on behalf of a company, your company) agree to use it solely for this purpose and subject to the terms of this Notice.

TI's provision of TI Resources does not expand or otherwise alter TI's applicable published warranties or warranty disclaimers for TI products, and no additional obligations or liabilities arise from TI providing such TI Resources. TI reserves the right to make corrections, enhancements, improvements and other changes to its TI Resources.

You understand and agree that you remain responsible for using your independent analysis, evaluation and judgment in designing your applications and that you have full and exclusive responsibility to assure the safety of your applications and compliance of your applications (and of all TI products used in or for your applications) with all applicable regulations, laws and other applicable requirements. You represent that, with respect to your applications, you have all the necessary expertise to create and implement safeguards that (1) anticipate dangerous consequences of failures, (2) monitor failures and their consequences, and (3) lessen the likelihood of failures that might cause harm and take appropriate actions. You agree that prior to using or distributing any applications that include TI products, you will thoroughly test such applications and the functionality of such TI products as used in such applications. TI has not conducted any testing other than that specifically described in the published documentation for a particular TI Resource.

You are authorized to use, copy and modify any individual TI Resource only in connection with the development of applications that include the TI product(s) identified in such TI Resource. NO OTHER LICENSE, EXPRESS OR IMPLIED, BY ESTOPPEL OR OTHERWISE TO ANY OTHER TI INTELLECTUAL PROPERTY RIGHT, AND NO LICENSE TO ANY TECHNOLOGY OR INTELLECTUAL PROPERTY RIGHT OF TI OR ANY THIRD PARTY IS GRANTED HEREIN, including but not limited to any patent right, copyright, mask work right, or other intellectual property right relating to any combination, machine, or process in which TI products or services are used. Information regarding or referencing third-party products or services does not constitute a license to use such products or services, or a warranty or endorsement thereof. Use of TI Resources may require a license from a third party under the patents or other intellectual property of the third party, or a license from TI under the patents or other intellectual property of TI.

TI RESOURCES ARE PROVIDED "AS IS" AND WITH ALL FAULTS. TI DISCLAIMS ALL OTHER WARRANTIES OR REPRESENTATIONS, EXPRESS OR IMPLIED, REGARDING TI RESOURCES OR USE THEREOF, INCLUDING BUT NOT LIMITED TO ACCURACY OR COMPLETENESS, TITLE, ANY EPIDEMIC FAILURE WARRANTY AND ANY IMPLIED WARRANTIES OF MERCHANTABILITY, FITNESS FOR A PARTICULAR PURPOSE, AND NON-INFRINGEMENT OF ANY THIRD PARTY INTELLECTUAL PROPERTY RIGHTS.

TI SHALL NOT BE LIABLE FOR AND SHALL NOT DEFEND OR INDEMNIFY YOU AGAINST ANY CLAIM, INCLUDING BUT NOT LIMITED TO ANY INFRINGEMENT CLAIM THAT RELATES TO OR IS BASED ON ANY COMBINATION OF PRODUCTS EVEN IF DESCRIBED IN TI RESOURCES OR OTHERWISE. IN NO EVENT SHALL TI BE LIABLE FOR ANY ACTUAL, DIRECT, SPECIAL, COLLATERAL, INDIRECT, PUNITIVE, INCIDENTAL, CONSEQUENTIAL OR EXEMPLARY DAMAGES IN CONNECTION WITH OR ARISING OUT OF TI RESOURCES OR USE THEREOF, AND REGARDLESS OF WHETHER TI HAS BEEN ADVISED OF THE POSSIBILITY OF SUCH DAMAGES.

You agree to fully indemnify TI and its representatives against any damages, costs, losses, and/or liabilities arising out of your non-compliance with the terms and provisions of this Notice.

This Notice applies to TI Resources. Additional terms apply to the use and purchase of certain types of materials, TI products and services. These include; without limitation, TI's standard terms for semiconductor products http://www.ti.com/sc/docs/stdterms.htm), evaluation modules, and samples (http://www.ti.com/sc/docs/sampterms.htm).

Mailing Address: Texas Instruments, Post Office Box 655303, Dallas, Texas 75265